



# UNIVERSITY OF BIRMINGHAM

Exhaust Gas Fuel Reforming To Achieve Fuel Saving

By  
Chin Pui Perry Leung

A thesis submitted to  
The University of Birmingham  
For the degree of  
Doctor of Philosophy

The University of Birmingham  
School of Engineering  
June 2012

UNIVERSITY OF  
BIRMINGHAM

**University of Birmingham Research Archive**

**e-theses repository**

This unpublished thesis/dissertation is copyright of the author and/or third parties. The intellectual property rights of the author or third parties in respect of this work are as defined by The Copyright Designs and Patents Act 1988 or as modified by any successor legislation.

Any use made of information contained in this thesis/dissertation must be in accordance with that legislation and must be properly acknowledged. Further distribution or reproduction in any format is prohibited without the permission of the copyright holder.

# Contents

ABSTRACT.....	5
Acknowledgements.....	7
Dedication .....	8
List of Abbreviations.....	9
CHAPTER 1 .....	12
1 Introduction.....	12
1.1 Background.....	13
1.2 Research Objectives.....	15
CHAPTER 2 .....	17
2 Literature Review.....	17
2.1 Spark Ignition (SI) engines .....	17
2.2 SI Combustion Process .....	22
2.3 SI Engine and Fuel Developments.....	28
2.4 Hydrogen Production Technologies.....	37
2.5 Hydrogen as Energy Carrier in Transportation .....	41
2.6 General Introduction to Catalytic Reforming .....	44
2.7 Benefits of Onboard Exhaust Gas Fuel Reforming .....	51

2.8	Exhaust Gas Reforming Routes .....	53
CHAPTER 3 .....		54
3	Experimental Setup .....	54
3.1	Reforming Catalyst .....	54
3.2	Reforming Rig.....	55
3.3	Exhaust Gas Emissions and Reformate Analysis.....	56
3.4	Fuel Properties .....	57
3.5	Calculation .....	58
3.6	Setup for Real Exhaust Gas Fuel Reforming (i.e. chapter 5).....	59
CHAPTER 4 .....		62
4	Catalytic Reforming of Ethanol .....	62
4.1	Testing Conditions .....	64
4.2	Reforming Testing Procedure.....	65
4.3	Results and Discussion.....	67
4.4	Chapter 4 Conclusions .....	83
CHAPTER 5 .....		85
5	Actual Exhaust Gas Reforming.....	85
5.1	Investigation into the Feasibility of Actual Exhaust Gas Reforming.....	85

5.2	Reforming Conditions.....	85
5.3	Results and Discussion.....	86
5.4	Chapter 5 Conclusion.....	91
CHAPTER 6 .....		93
6	Partial Gasoline Replacement by Simulated Reformate .....	93
6.1	The Effect of Simulated Reformate (CO + H <sub>2</sub> ) as Fuel Replacement on Engine Performance.....	93
6.2	Reformate Properties.....	93
6.3	Testing Procedure and Conditions .....	94
6.4	Engine Fuel Replacement Calculation.....	99
6.5	Engine out Emissions.....	104
CHAPTER 7 .....		108
7	Summary .....	108
8	LIST OF PUBLICATIONS.....	114
9	REFERENCES.....	116

# ABSTRACT

As much as 70 to 75% of the energy in the fuel used by a car is turned into waste heat, with more than a third of this released through the exhaust pipe. Catalysis offers a way of recovering exhaust heat. By adding some of the fuel to a portion of the exhaust as it passes through a catalytic reactor, it is possible to produce a gas mixture with a higher heating value than the fuel. This strategy depends, however, on the catalytic reaction consuming heat, while generating readily-combustible products that can be fed back to the engine.

An investigation into catalytic exhaust gas fuel reforming and its potential to improve engine emissions and efficiency when close-coupled to a spark ignition engine.

Initial ethanol reforming reactions with simulated exhaust gas suggests that the desired reforming path, i.e. dry reforming, steam reforming and partial oxidation reforming reactions can raise the heating value of the input fuel (ethanol) by up to 120% providing exhaust gas temperatures are made available, with the highest being steam reforming > dry reforming > oxidative reforming. The undesired water gas shift reaction is inactive with this reforming catalyst, regardless of the reaction temperature and reactant ratios (e.g. O:C and H<sub>2</sub>O:C). The characteristic of each reforming path is tentatively explained with deviations from the stoichiometry.

Actual exhaust gas fuel reforming studies of gasoline is carried out at a range of

exhaust gas temperatures. It was found that at exhaust gas temperature 600° to 950°C, the overall process efficiency ranges from 107 to 119%.

By replacing 23.9% of gasoline fuel with simulated reformat, improvements in engine specific fuel consumption (SFC) and emissions (e.g. NO<sub>x</sub>, HC, CO<sub>2</sub>, CO) was achieved.

# **Acknowledgements**

I would like to thank Dr. Tsolakis A. and Professor Mirosław L. Wszyński for their help and guidance during my PhD course, it was greatly appreciated.

Thanks go to Johnson Matthey, Shell Global Solutions UK and Jaguar Land Rover for their support and help with the supply of hardware.

***This thesis is dedicated to***

*My Grandmother - Y.O. Wong*

*My family - W.F. Lam, K.M. Leung, C.H. Leung, T.Y. Leung;*

*My girl friend - S. Ong*

*My beloved friends – Ho Nam, Chung, B.K., W.Y., Fire, Gar, Tom, Wests...etc*

*For their endless love, support and encouragement.*

## List of Abbreviations

$AFR_{\text{Stoich}}$	Stoichiometric Air to Fuel Ratio
ATR	Autothermal Reforming Reaction
Adv	Advanced
BEPV	Battery Electric Powered Vehicle
CAD	Crank Angle Degrees
$CH_4$	Methane
CI	Compression Ignition
CO	Carbon Monoxide
$CO_2$	Carbon Dioxide
COV	Coefficient of Variation
CR	Compression Ratio
$C_2H_6O$	Ethanol
DDR	Dry Reforming Reaction
DI	Direct Injection
DMF	2,5 Di-methylfuran
DOC	Diesel Oxidation Catalyst
DPF	Diesel Particulate Filter
$E_{xx}$	$xx\%$ Ethanol volume concentration in gasoline
EGR	Exhaust Gas Recirculation
EOI	End of Injection
FBP	Final Boiling Point
FCEPV	Fuel Cell Electric Powered Vehicle

FCHPV	Fuel Cell Hydrogen Powered Vehicle
GDI	Gasoline Direct injection
GHSV	Gas Hourly Space Velocity
GTL	Gas To Liquids
H	Hydrogen
H <sub>2</sub> O	Water
HC	Hydrocarbons
HO	Hydroxide
HCCI	Homogeneous Charge Compression Ignition
IBP	Initial Boiling Point
IMEP	Indicated Mean Effective Pressure
$\lambda$	Relative Air-Fuel Ratio
MBT	Minimum advance for Best Torque
MFB	Mass Fraction Burned
MON	Motor Octane Number
MTBE	Methyl Tert-Butyl Ether
N	Nitric
N <sub>2</sub>	Nitrogen
NO	Oxide of Nitrogen
NO <sub>x</sub>	Oxides of Nitrogen
O	Oxygen
TDC	Top Dead Centre
PFI	Port Fuel Injection
PM	Particulate Matter
POX	Partial Oxidation Reaction

Pt	Platinum
Rh	Rhodium
Rtd	Retarded
RME	Rapeseed Methyl Ester
RON	Research Octane Number
RPM	Engine speed, Revolutions per Minute
RVP	Reid Vapour Pressure
$Q_{in}$	Heat input
$Q_{out}$	Heat output
$W_{in}$	Work input
$W_{out}$	Work output
$W_{net}$	Work output - Work input
SCR	Selective Catalytic Reduction
SFC	Specific Fuel Consumption
SI	Spark Ignition
SoC	Start of Combustion
SoI	Start of Injection
SRR	Steam Reforming Reaction
ST	Spark Timing
Std	Standard
$\eta_{th}$	Thermal Efficiency
ULSD	Ultra Low Sulphur Diesel
VCT	Variable Cam Timing
VOCs	Volatile Organic Compounds
WGS	Water Gas Shift

# CHAPTER 1

## 1 Introduction

Despite the constant development of the internal combustion engine technology since the 19th century, the problems associated with the environmental pollution and health hazards have only been recognised in recent years. Some of the developed countries (including the EU, USA and Japan) have introduced legislations in order to control emissions from transportation. The global road fleet of 750 million cars produces 5000 metric tons of carbon dioxide per year (ITF, 2010). In excess of 3000 metric tons of these emissions can be attributed to the inherent inefficiency of the internal combustion engine, which radiates heat, requires cooling and braking, and releases hot exhaust gas into the atmosphere. Each of these sources of inefficiency is currently being addressed in the universal push towards higher fuel economy and lower CO<sub>2</sub> emissions. Among the most challenging is the recovery of waste heat from the exhaust, with mechanical and thermoelectric technologies reported by (Messerer et al., 2007) and (Lee et al., 2010) respectively showing most promise. However, exhaust gas reforming technology – which provides a chemical route to heat recovery – should be considered as a serious contender. In terms of decarbonisation of primary fuel, hydrogen has been foreseen as the long term sustainable energy solution. Nevertheless whether a defining hydrogen economy is feasible relies upon the current storage (Aardahi &

Rassat, 2009), production (Holladay et al., 2009) and existing infrastructure technologies (Agnolucci, 2007) of the transport sectors.

## 1.1 Background

### 1.1.1 Exhaust Gas Fuel Reforming in CI Engines

The actual engine exhaust gas temperature (e.g. 180° to 450°C) in CI engines is usually below that required in the desirable endothermic reactions of SRR and DRR. This absence of temperature can be resolved and the endothermic reactions can be sustained as under lean exhaust gas conditions, the oxygen part of the exhaust reacts with a portion of fresh fuel to raise the temperature. This exothermic reaction generates heat along the catalyst bed and provides the temperature needed for the endothermic reforming reactions. A main drawback of this process at low exhaust gas temperatures is an increase in fuel consumption. For this reason, applications of this technology are mainly focused on enhancing aftertreatment devices' performance in reducing emissions by using small quantities of hydrogen (e.g. 1000ppm H<sub>2</sub>).

### 1.1.2 Exhaust Gas Fuel Reforming in Spark Ignition Engines

Stoichiometric combustion ( $\lambda$  proximately 1) of SI engines limits the oxygen presence in the exhaust stream (at typically ~1% vol.). This implies the reforming

temperature cannot rely on the partial oxidation reaction. Nevertheless, the exhaust gas temperature is substantially higher in comparison with CI engines. When SI engines are under high IMEP operating conditions, knock is a constraint.

Providing the reactions taking place in the reformer are net endothermic, the process will have the combined and inter-related effects of recovering heat, increasing the heating value of the fuel, even though the fuel conversion is not complete. By re-circulating the reformat back into the engine as a fuel replacement (Figure 1-1), it has the potential to improve engine fuel economy (i.e. SFC) and reduce CO<sub>2</sub> emissions.

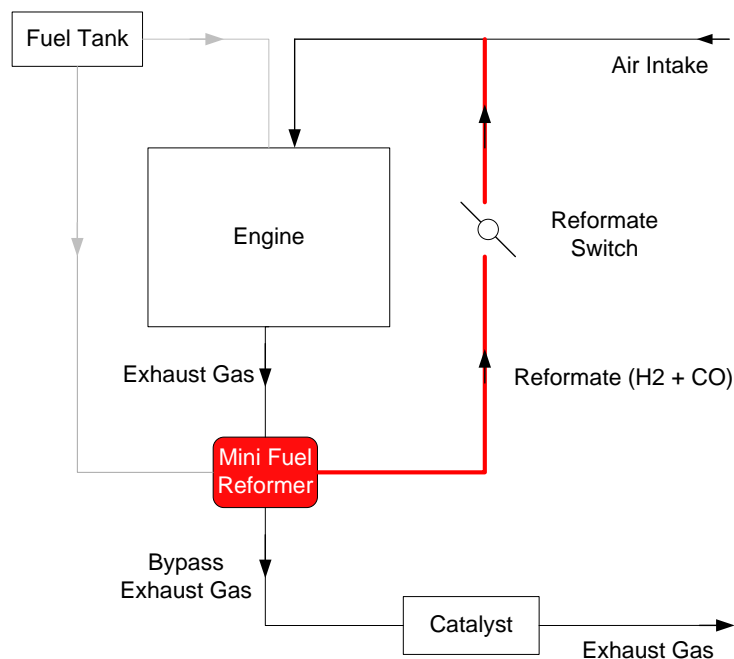


**Figure 1-1 Schematic diagram of reformer close-coupled with SI engine, with reformat being fed back to engine intake.**

## 1.2 Research Objectives

The research presented in this thesis was conducted at the University of Birmingham with support from Johnson Matthey and Shell Global Solutions UK.

The objective of this research is to develop a more fundamental understanding of the catalytic fuel reforming and the feasibility of the exhaust gas fuel reforming technology to achieve simultaneous fuel saving and emissions reductions in SI engine. The research splits into four parts, equilibrium calculations to predict fuel savings in SI engine, catalytic fuel reforming studies, actual exhaust gas fuel reforming studies and combustion studies with reformat additions.

In more detail, the main objectives of this study were:

Based on a selected range of engine exhaust gas conditions, the first part of this study used chemical equilibrium software to predict the feasibility of fuel savings in the case of close-coupled exhaust gas reforming conditions.

Second part of the study assesses the Rh-based catalyst performance, targeting selectivity of individual reforming reactions and their operation windows. The potential of raising the heating value of reformates is also investigated. Utilising ethanol at to represent HC-type fuel at this part of the study minimises the amount of complex reactions which may complicate the analysis.

Thirdly, the actual exhaust gas reforming part of the study investigated the performance of a reforming catalyst under SI engine exhaust gas conditions fuelled with gasoline. The potential fuel saving is predicted based on the reformer performance.

Fourthly, simulated closed-loop reforming replaced part of the primary fuel (gasoline) with simulated reformat. The combustion and emissions performance is compared against standard engine setup.

The combustion studies were conducted on a single cylinder direct injection spark ignition research engine, representative of a multi-cylinder (V8) engine.

# CHAPTER 2

## 2 Literature Review

### 2.1 Spark Ignition (SI) engines

The wide use of the spark ignition (SI) engine vehicles has dominated the global automobile market share and is attribute to good engine performance, good infrastructure availability, lower tail-pipe emissions (soot), cost effectiveness for manufacture and emissions treatment. Problems related to the thermal efficiency (typically 25% for a SI engine), lower fuel economy and higher CO and NO<sub>x</sub> emissions (than CI engines) continues to improve with engine development (e.g. improved combustion system design). Its combustion process has been extensively studied over the years by researchers with the shared aim to improve brake specific fuel consumption and to comply with future emissions legislation. The work presented here was focused on further improving the thermal efficiency of SI engines via onboard fuel reforming technologies.

#### 2.1.1 SI Engine Emissions

It is generally known that the combustion of fossil fuels contribute a significant amount of global emissions, i.e. CO<sub>2</sub>, CO, NO<sub>x</sub>, unburned-HC. The first recorded pollution regulatory policy was established by Edward I of England (1272-1307) in the thirteen

century, protesting the dark smoke by burning ‘sea coal’ while the king was in town. However, extensive literatures regarding the mechanism of emission formation in SI combustion was not available until recent decades. Factors such as engine design (i.e. air flow motion, swirl), combustion speed and compression ratio effect the types of emissions present. Complete combustion helps reduce the amount of harmful substances. Precise control of spark timing, injection process and optimum air:fuel ratio have a direct impact on complete combustion. An overview of SI emissions trends with relative air-fuel ratio has been reported by (Harrington & Shishu, 1973), this general trend still describe the modern spark ignition engine well, see Figure 2-1. Details of these regulated emissions are discussed in the following section.

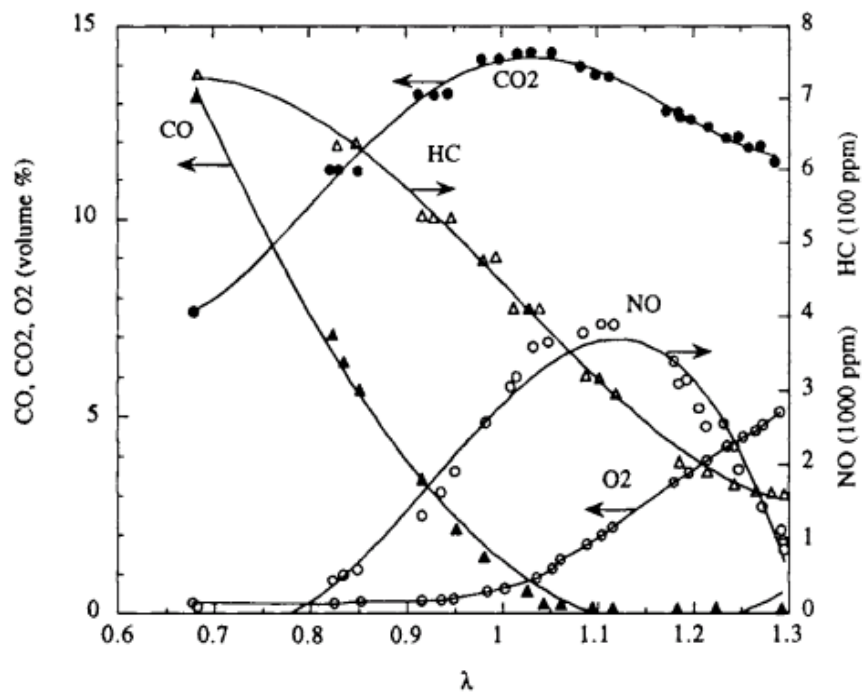


**Figure 2-1 variation of engine out emissions with relative air-fuel ratio (Harrington & Shishu, 1973).**

## 2.1.2 Unburned Hydrocarbon -HC

Exhaust gas from an SI engine can contain up to 6000 ppm of HC, (equivalent to 1-1.5% of the input fuel). Approximately 40% of this HC emission originates directly from the gasoline fuel, the rest are intermediate compounds formed during the combustion process (Pulkrabek, 1997). HCs can be formed from a number a sources. (Cheng et al., 1993) have compiled a comprehensive report from a range of studies and they proposed several HC formation pathways for SI engine combustion, see Figure 2-2. The tailpipe HC emissions can form through) i) in-cylinder oxidation, ii) exhaust oxidation, iii) catalyst oxidation. Each source of hydrocarbons is represented as a percentage of the total fuel HC. (Cheng et al., 1993) also concluded that the unburned HC is a direct result of incomplete combustion, with air:fuel ratio having a strong influence on HC formation. Lean combustion allows a higher oxygen availability to react with a unit fuel atom, thereby reducing the chance of unburned HC.

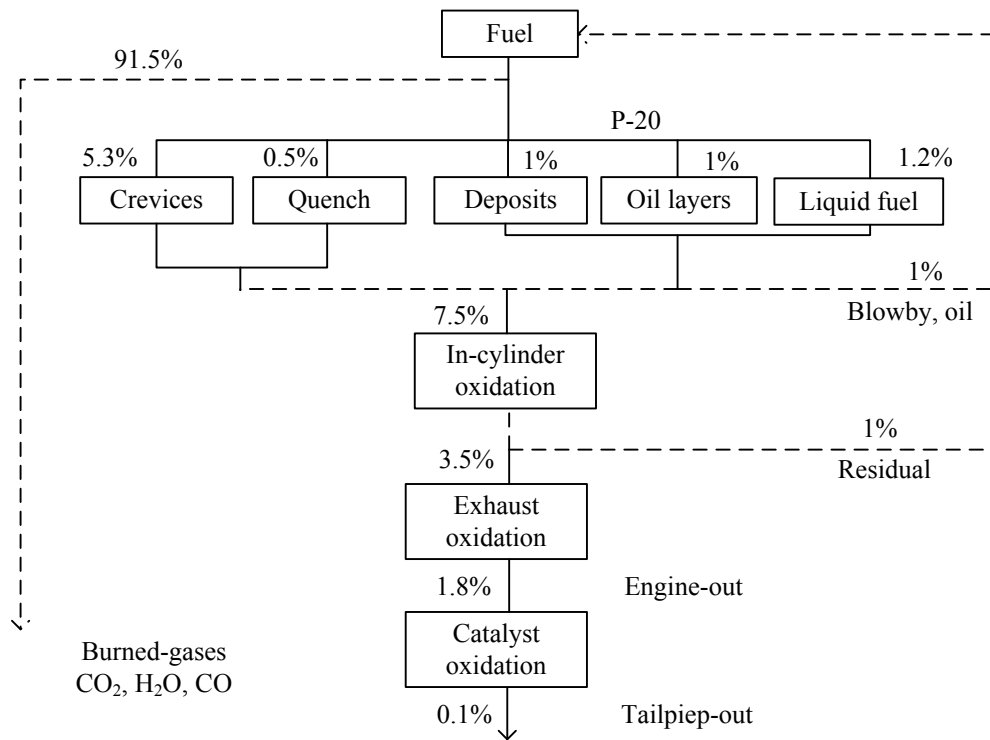
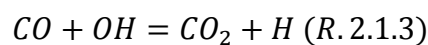


**Figure 2-2 Estimated magnitudes of HC formation sources during medium speed and load. (Cheng et al., 1993)**

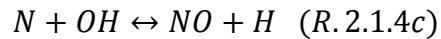
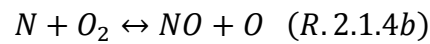
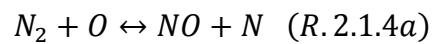
### 2.1.3 Carbon Monoxide-CO

The formation of CO emissions is generally accompanied by unburned HC due to the sensitivity to the air:fuel ratio (e.g. in the case of hard acceleration and engine cold start). For the same reason, CO formation is at maximum within the combustion chamber near the flame zone, it is lower in the exhaust gases but still significantly higher than equilibrium adiabatic combustion (Heywood, 1989). If enough oxygen is present, CO should oxidise with OH particles to produce more CO<sub>2</sub> and H.



## 2.1.4 Oxides of Nitrogen-NO<sub>x</sub>

Nitric oxide (NO) and nitrogen dioxide (NO<sub>2</sub>) are commonly described by a collective term (NO<sub>x</sub>). The NO formation paths are mainly governed by the Zeldovich mechanism, reported by (Zeldovich, 1947).



### **R. 2.1.4 Zeldovich mechanism of NO<sub>x</sub> formations (Zeldovich, 1947).**

The strong triple bonded N<sub>2</sub> molecule shown in R. 2.1.4, requires high activation energy in order to break free. It is evident from chemical kinetics that the rate of NO formation is exponentially dependent on flame temperature. Typically a high combustion temperature of 2000K, is required to significantly promote the rate of this reaction. This would imply that the increase of compression ratio, injection pressure, turbo boost pressure and rich mixture should lead to high NO<sub>x</sub> formation. Under lean mixtures, the duration of combustion would also increase NO<sub>x</sub> formation via the extended exposure period of high combustion temperature (Stone, 1999). The turbulence and the amount of excess oxygen are two other important factors of the NO<sub>x</sub> formation.

### 2.1.5 Carbon Dioxide-CO<sub>2</sub>

CO<sub>2</sub> emissions from fuel combustion is one of the most significant greenhouse gas contributors (IEA, 2010). It is perhaps bizarre that increased CO<sub>2</sub> in combustion signifies a more complete (clean) combustion. In reality, the specific unburned HC and CO emissions are reduced with improves combustion efficiency; therefore one of the primary CO<sub>2</sub> reduction methods is to improve the overall engine efficiency or alternatively reduce the carbon content of fuel.

## 2.2 SI Combustion Process

Different combustion analysis techniques such as in-cylinder pressure measurements, is commonly used to monitor and analyse the combustion process. In 4-stroke SI engines, stoichiometric air:fuel mixture is drawn-in the cylinder during the induction stroke. The combustion process initiates by a spark discharged toward the end of the compression stroke, Figure 2-3. Whereby high temperature plasma generates by the spark develops into exothermic reactions which propagate across the unburnt air:fuel mixture. It then extinguishes and escapes from the exhaust valve at end of the expansion stroke. The spark timing can significantly alter the combustion phase; therefore it is often used to control primarily the maximum power output. For late ignition timing, there may be a risk of incomplete combustion before the exhaust valve opens, especially under high speed

combustion where the residence time per unit mass of fuel is significantly reduced.

The early combustion period comprises the initial laminar phase combustion and transfers into fully turbulent phase combustion. The delay between these depends on the temperature, pressure and the composition of the air:fuel mixture. This early combustion period is commonly calculate by the pressure trace histories, and represent by the 0 to 10% MFB for the lamina phase, and 10 to 90% for the turbulent phase. At the final stage of the combustion process (i.e. >90 % MFB), the reduced contact between unburnt gas mixture and the flame front area cause the reminding unburnt hydrocarbon:air mixture to burn slower (Stone, 1999). These unburnt mixtures at the crevices often leave the exhaust port without reacting, making up the inefficiency of the combustion process with evidence of unburnt hydrocarbons.

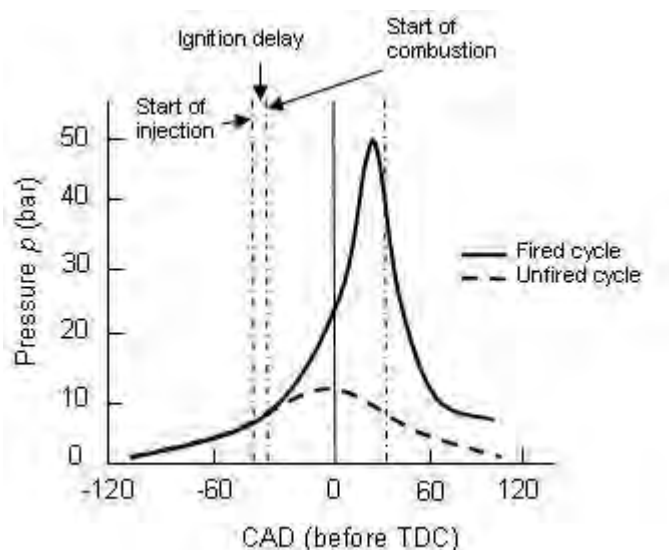


**Figure 2-3 SI engine cylinder pressure diagram**

## 2.2.1 What Thermal Efficiency Can Otto Achieve?

Ideal Otto cycle is typically used to describe an ideal SI combustion process, assuming a constant volume heat addition and adiabatic expansion environment. Figure 2-4 and 2-5 illustrates that for an equal compression and expansion stroke, piston cannot return to its intake pressure without exhausting heat. For this reason, heat engine can never achieve 100% thermal efficiency.

$$Q_{in} + W_{in} = Q_{out} + W_{out} \quad (\text{Eq. 2.1a})$$

$$Q_{in} - Q_{out} = W_{out} + W_{in} \quad (\text{Eq. 2.1b})$$

$$Q_{in} - Q_{out} = W_{net} \quad (\text{Eq. 2.1c})$$

$$Q_{in} - Q_{out} = Q_{in} \times \eta_{th} \quad (\text{Eq. 2.1d})$$

$$Q_{in} \times (1 - \eta_{th}) = Q_{out} \quad (\text{Eq. 2.1e})$$

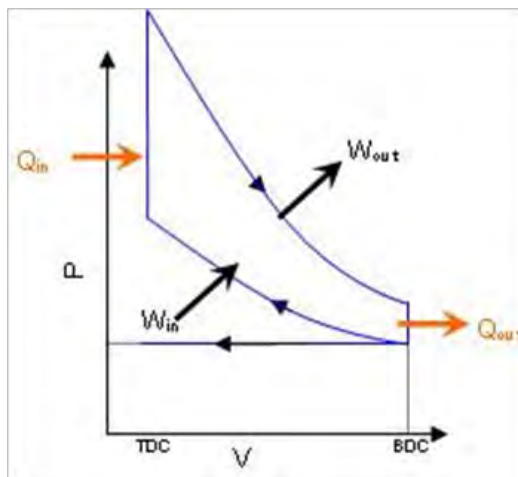


**Figure 2-4 Pressure -Volume diagram of ideal Otto cycle**

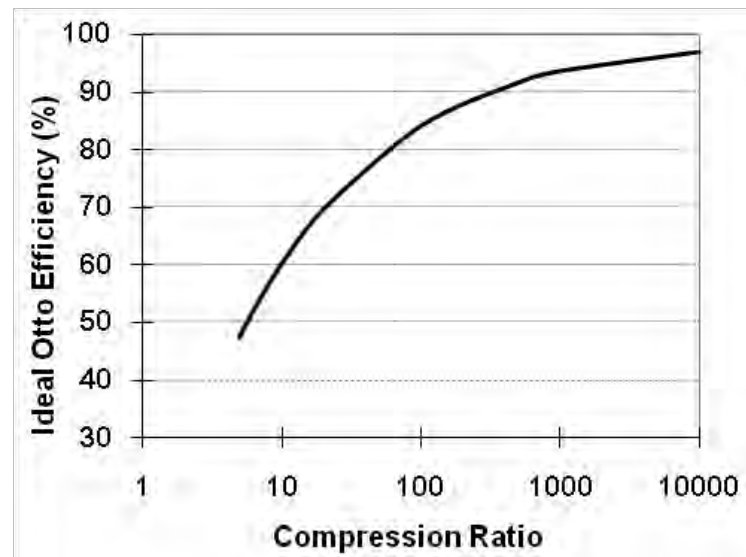


**Figure 2-5 Ideal Otto cycle efficiency versus compression ratio diagram**

$$\eta_{th} = 1 - r^{1-\gamma} \text{ (Eq. 2.1f)}$$

Where:  $\eta_{th}$  - thermal efficiency

r - compression ratio (cylinder volume ratio of TDC over BDC)

$\gamma$  - specific heat ratio at constant pressure and volume ( $C_p/C_v$ )

The theoretical Otto cycle's thermal efficiency is limited largely by the engine compression ratio. This is because in cylinder temperature and pressure is governed by the engine compression ratio. The higher the combustion temperature, the less likely that incomplete combustion occur, thus higher the thermal efficiency. However, this increased end gas temperature and density associated with this pressure rise can cause air-fuel mixture pre-ignition prior to spark plug fires, i.e. "knocking", causes reduce in power and damage to piston. The maximum thermal efficiency of an ideal Otto cycle at a typical CR of 10 is 60%.

## 2.2.2 What Thermal Efficiency Can SI Engine Achieve?

In practice, SI engines can hardly achieve half of theoretical thermal efficiency value. This is because in actual SI cycle, spark timing does not always happen at TDC and actual burning process takes a finite time (NB: also depending on flame speed of fuel and compression ratio), thus the constant volume process is not a valid assumption. (Kikuchi et al., 2003) reported that in piston sealing's friction associated with increase cylinder bore temperature, i.e. compression ratio associated. For these reasons, engine oil and coolant is necessary to ensure a proper engine operation, mechanical reliability and most importantly to promote in cylinder volumetric efficiency. This means the adiabatic expansion process can never be achieved in the expansion stroke either, see Figure 2-6. As a consequence, actual thermal efficiency is further limited to 15 to 32%, which vary in different engine design and operation.

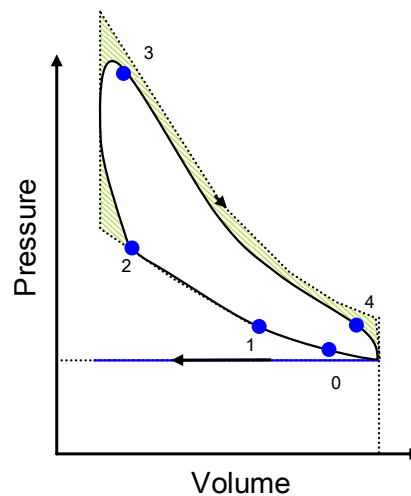


**Figure 2-6 Thermal efficiency diagram of 4-stroke engine**

### 2.2.3 Fuel to Heat Rejection

Knowing a large proportion of fuel energy is dissipated in heat during the combustion process, it is necessary to locate and quantify these fuel inefficiencies. The large number of engine dependant variables and engine design variability makes precise heat rejection data difficult to compare. (Chammas and Paris, 2005) have reported heat rejection data of a light duty gasoline spark ignition engine with respect to fuel energy percentage. Of which, the energy released to radiator and exhaust gases attributed 18 to 42% and 22 to 46% of the fuel energy input respectively. This is due to the much higher exhaust gas temperature (up to 900°C) and the emissions in exhaust gas (i.e. HC, CO, CO<sub>2</sub>, and H<sub>2</sub>O) containing energy. In the exhaust the wasted or unutilised energy when translated into kW it ranges from 4.6 to 120 kW, which is significantly higher than that in the coolant where it ranges from 9 to 48 kW. Similar heat rejection figures to exhaust and radiator from an 180kW SI engine was published in a report by (Martins et al., 2011), and exhaust gas temperature up to 1000°C has been observed by the author. See Figure 2-7 for the energy flow diagram summary. There are number of existing technologies to recover part of these losses, later discussed in Chapter 2.

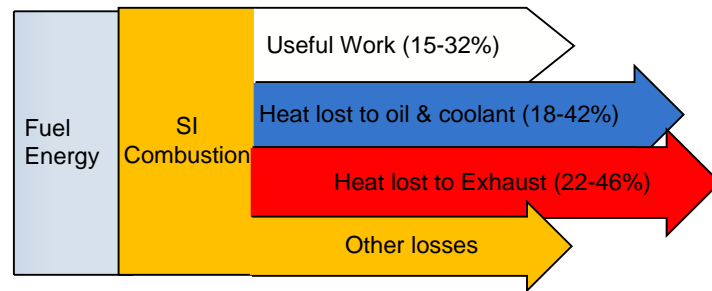


**Figure 2-7 Fuel energy flow chart of SI engines**

## 2.2.4 Volumetric Inefficiency

In CI engines, the maximum air mass flow is always drawn into the combustion chamber (regardless the AFR) while the mass flow of fuel is used to control the engine torque output and therefore the volumetric efficiency is typically high as 90%. In SI engines, the combustion process occurs at a relatively homogenous condition, fuel can neither burn efficiently with excess or too little air. The load control of SI engines utilise throttle valve to alter the intake charged density. This method provides simplicity and responsive transient behaviour, but the pressure difference across the intake valve induces pumping losses. The volumetric efficiency of a naturally aspirated SI engine can vary between 90% at high engine loading down to 15% at part-engine loading. (Ferguson & Kirkpatrick, 2001), highlighted a clear correlation between intake:exhaust pressure ratio to thermal efficiency. In their findings, thermal efficiency can be significantly reduced by 20% when the throttle position is reduced from 1.0 to 0.3 (value range from 0 to 1 correlate to the throttle position from fully closed to fully opened). Modern SI engine utilises exhaust gas recirculation at low speed conditions,

where intake flow is most restrictive, throttling effect can be reduced. Utilising EGR can reduce this pressure differential, but is known to associate with increased engine-out HC and smoke due to the lower combustion temperature and slower combustion.

## 2.3 SI Engine and Fuel Developments

Knowing SI engines have the potential of doubling its existing efficiency, on-going research continues to explore various technology routes toward this limit. Bear in mind with constraints such as emissions legislation, production cost, geographic and existing infrastructure, the following categories should be higher up the priority list;

i) ***Improve fuel properties*** – reformulate gasoline fuel properties, aim to improve thermal efficiency via extending CR. Reformulated fuel should contain lower carbon content such that overall emissions could simultaneously reduce.

ii) Engine ***Heat rejection recovery*** – significant fuel energy is wasted as heat rejection to coolant and exhaust. At present, only part of these losses are being recovered via cabin heating and turbo-charging. Technologies to recover exhaust energy as thermal-electric energy is under development, but conversion efficiency is yet to be discovered.

iii) ***Gasoline Direct injection (GDI)*** - this technology works by injecting fuel directly into the combustion chamber during the compression stroke with precise control of fuel quantity and timing. This enables the engine to also operate beyond stoichiometric operating

condition, i.e. ultra lean at light load, rich at high load, which promotes complete combustion and reduced pumping losses. In practice this technology has a cost implication due to higher injector standard as it has to withstand the higher combustion temperature, higher onboard computer processing speed, and additional NO<sub>x</sub> aftertreatment for the lean exhaust conditions. Therefore this may not be justified for normal operating automobiles.

iv) downsized turbocharged engine – is a technology that offers substantial specific fuel consumption improvement over conventional natural aspirated engines. It is achieved by turbo charging an engine with smaller engine displacement volume; so that for a given power output the downsized turbocharged engine can always operate at a higher mean effective pressure. Study by (Milpied et al., 2009) reported that the axial losses such as pumping, mechanical friction and heat transfer are spontaneously reduced. On the other hand, controlling knock is the major challenge as the engine operates at higher cylinder pressure.

### 2.3.1 Improve Fuel Quality

Retarding spark timing to compromise a high CR ratio can incur a power penalty. Alternatively, blending regular gasoline with higher octane fuel can extend the knock limit for a given compression ratio. The following sections discuss the pros and cons of different blending options.

### 2.3.2 Lead and Methyl Tertiary Butyl Ether (MTBE)

The addition of tetraethyl lead  $(C_2H_5)_4Pb$  was commonly used to enhance the octane value of gasoline fuel since the early 1920's, it's to allow the SI engine to operate at a higher compression ratio and hence a higher specific engine power output without the influence of 'knock'. Lead additive is also known to control surface ignition and reduce carbon deposits on valves therefore reduce incomplete combustion. The used of lead as a fuel additive has gradually phased out after Philip J. Landrigan and his team (1976) revealed the harmful effects to human neurologic system. Furthermore, the used of  $(C_2H_5)_4Pb$  has the tendency to poison aftertreatment catalyst (Heywood, 1989).

### 2.3.3 Methyl tert-butyl ether (MTBE)

Using MTBE, i.e. a mixture of ethers, as an additive became popular after the phase out of tetraethyl lead as it could compensate for the lowered octane due to reduced aromatic fuel content. Beside, (Nadim et al., 2001) and (Taljaard et al., 1991) reported that MTBE significantly reduces CO, NO<sub>x</sub> and HC emissions at stoichiometric A:F ratio. (Andrews et al., 1988) conducted a study with different MTBE content in gasoline. Of which, he concluded that the reduction of CO is mainly attribute to the reduced aromatic content of MTBE, where reduction of NO<sub>x</sub> at part load condition is due to the volatility behaviour of oxygenated content.

Despite the growing concerns that MTBE has a toxicity effect as a drinking water on human/animals and it has been detected over ground and drinking water in the US. (EPA, 1997) has stated that further investigation is required in order to re-access the potential health and environmental impact.

### 2.3.4 Bio-Ethanol

Despite the uncertainties and on-going food versus fuel production debate, significant funds have been invested into biofuel development as a way to meet short and long term CO<sub>2</sub> reduction target (EPA, 2010); (COM, 2012); (APEC, 2008); (Masaki & Asia Times, 2007). Brazil for example is one of the pioneering countries of bio-fuel development of which 8 out of 10 on-road vehicles are bio-fuel compatible, and 20% of its automotive petroleum is substitute by its self-sustained ethanol (Hira & Oliverira, 2009).

As a fuel additive, EPA has recently granted permission to increase the ethanol content in gasoline to 15%, known as E15 (EPA, 2011), while EU's directive expect E10 to phase in after 2013 (2009/30/EC, 2009).

The main advantage that ethanol offer over gasoline as a fuel is the high RON value of 129 when compared to regular gasoline of 84, which stand for a higher knock resistance. Replacing a portion of gasoline with ethanol can therefore improve specific fuel consumption via extended cylinder pressure limit before pre-ignition occurs. (Piel & Thomas,

1990) reported that, by adding 1% weight of ethanol into gasoline, it enhances Reid Vapour Pressure - RVP by approximately 6.9 kPa, (Figure 2-8). NB: the higher the RVP the more volatile the liquid and the more readily it will evaporate, see (ASTM). Another study by (Sodre & Sordre, 2011) concluded that when an engine is fuelled by gasoline-ethanol blend and hydrous ethanol fuel, significant specific fuel consumption and thermal efficiency improvement has been reported attributed to the extended upper compression ratio limit. Up to 17% SFC improvement has been reported with E60 over conventional gasoline (Kuroda et al., 2006). A government study reported that mixing alcohols (including ethanol and methanol) in gasoline enhanced gasoline octane rating and therefore significantly reduced engine emissions substantially (UCTC & WVU, 1991-1998).

On the down side, (Szybist et al., 2010) compared the combustion performance of regular gasoline and E15, i.e. 15% ethanol-gasoline blended. Of which, the E15 has shown a 9.5% IMEP improvement over the regular gasoline at a fixed inlet throttle pressure of 80 kPa. This improvement however is not sufficient to compensate the reduced energy content of E85, results an increased ISFC from 244 g/kWh for regular gasoline to 338 g/kWh for E85. Besides, the low vapour pressure is known to cause engine start problem during cold weather conditions. Moreover, significant advance in injection timing could occur depending on the ethanol to gasoline mixing ratio, a high mixing ratio could cause a sharp increase in in-

cylinder pressure. For these reasons, automotive manufacturers have defined their warranty and are limiting the allowable ethanol to gasoline mixture on conventional gasoline powered vehicles. A research attempt by (Rounce et al., 2009) has been reported to reformulate a mixture of bio-fuel so that such can fuel performs on the engine without altering the engine setting.

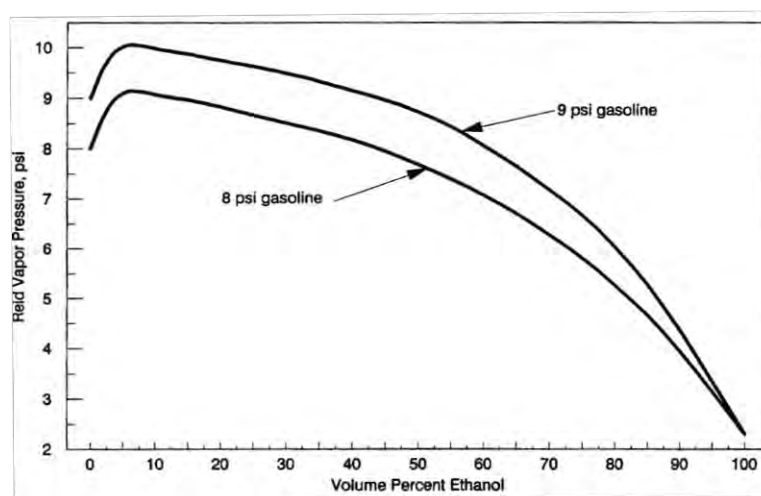


**Figure 2-8 Percentage of gasoline-ethanol blend vs. RVP (API, 1988); Re-distributed by (www.tpub.com)**

### 2.3.5 Hydrogen

Following the Organisation of Arab Petroleum Exporting Countries - “OAPEC” oil crises back in 1973, hydrogen as a carbon-free element has become the primary focus of fossil fuel alternatives. Partly due to the fact that hydrogen is the most abundant element in the universe, comprises 75% of our environment. Besides, it has excellent combustion characteristic such as high octane number, heating value, minimum ignition energy and the

fact that it produces zero emissions when combusted with oxygen makes hydrogen an ideal fuel.

Table 2-1 highlights the important properties of hydrogen among other fuels. (Edwards et al., 2008) concluded that "despite the pronounced benefits of hydrogen combustion, technical barriers related to its production and storage are yet to be resolved and make hydrogen competitive with conventional fuels."

(Kito et al., 2000) studied the ignition limits of hydrogen using the flame jet ignition method, in a combustion chamber at CR of 8.8. They concluded that the engine was able to maintain an ultra-lean combustion with an equivalence ratio of 0.34 due to the wide flammability limit of H<sub>2</sub> when compared to gasoline. In another study by (Kee et al., 2007) the effect of hydrogen addition on knock characteristics using a rapid compression/expansion machine were investigated. They concluded that when H<sub>2</sub> is added to gasoline as a fuel additive, it reduced knock intensity and allowed the engine to operate at higher CR (or avoid spark timing retard from MBT), hence improving engine efficiency and reducing emissions. (Alger et al., 2007) also reported that due to the increased burning velocity of H<sub>2</sub>, a small amount of H<sub>2</sub> (0.2 vol.%) is able to stabilize the engine while it was operating at its maximum EGR limit; and with 1 vol.% H<sub>2</sub> enrichment, the EGR limit was extended from 27 to 50%.

Furthermore, (Shinagawa et al., 2004) compared the flame propagation between gasoline and hydrogen addition on a modified transparent engine. In which, they have concluded that hydrogen addition increased the burning velocity via all stages of flame propagation, and is an ultimate solution to knocking. In the same study, he justified that the same hydrogen effect can be achieved by intensifying the turbulence of gasoline fuelled combustion model.

On the contrary, the reduced quenching distance of  $H_2$  allows flame to travel closer to the cylinder wall and passes via a closing valve, hence increases the chance of back firing (Glassman, 1996). Furthermore, the MBT spark timing will certainly be advanced with accordance to the amount of substitute fuel, unless additional fuel with the opposite fuel properties, i.e. slow burning velocity, that attribute a cancelling effect.

**Table 2-1 Fuel properties**

Properties	Fuel			
	Hydrogen	Gasoline	Methane	Ethanol
Molecular weight	2.016	114.2	16	46
Density (kg/m <sup>3</sup> )	0.0838	791	0.72	
Boiling temperature (deg.C)	-252.8	37-204	-116	
Kinetic viscosity (m <sup>2</sup> /s)	1.60E-07	0.8	3.30E-07	
Diffusion coefficient in still air (cm <sup>2</sup> /s)	0.61	0.05	0.16	
Quenching distance (mm)	0.6	2.84	2.1	
Stoichiometric A:F ratio	34.2	14.7	17.3	9
Lean Limit equivalence ratio	0.1	0.58	0.5	
Flammability in air (%vol.)	4-75	1-7.8	5.3-15	3-19
Minimum ignition energy (mJ)	0.02	0.24	0.29	
Minimum autoignition temperature at stoichiometric (K)	858	500-744	813	-600
Adiabatic flame temperature in air at stoichiometric (K)	2318	2148	2470	
Maximum flame speed in air (m/s)	2.8	0.37-0.43	0.37-0.45	
Net energy density (MJ/m <sup>3</sup> )	10.3	202	34.2	
Lower heating value (MJ/kg)	120	44	50	27
Octane number	>130	87-100	120-130	108
Reid vapour pressure (psi)		8-15	4.6	2.3

## 2.4 Hydrogen Production Technologies

While over 80% of the global power sources is powered by combustion of fossil fuel (IEA, 2010), it has been estimated that from the present consumption rates, the known oil resources will last approximately 40 years (Agarwal, 2007). Whereby sustainable alternative energy resources must be developed and be adapted.

A comprehensive study from a range of sustainable energy developments stated that, the majority of the invested alternative energy technologies are inconsistent and are under-developed (Lior, 2010).

Specifically in transportation sector, it seems that major automotive companies are investing heavily in battery powered electric (BEPV), fuel cell electric vehicles (FCEPV) and fuel cell hydrogen vehicles (FCHPV) to achieve the so called 'carbon-free' vehicles (IMEng, 2009). While quantitative studies suggest that BEPV, FCEPV and FCHPV could achieve lifecycle cost parity or lower than conventional gasoline powered vehicles by 2030 (Offer et al., 2010), there are a number of technical barriers to be resolved. For example, (Anderman, 2007) reported that the battery life span, energy density (e.g. Li-ion 180 Wh/kg) and the driving range versus production cost of BEPV are far from economically friendly. It is likely that fuel cell technologies and plug-in hybrid vehicles are more likely to co-exist with IC engines (gasoline & diesel) until the end of fossil fuel use. In the mean while a substantial carbon neutral fuel is needed as most alternative energy technologies are far from commercially/economically available.

Despite hydrogen not existing in nature and only appearing in compounds, i.e. water (H<sub>2</sub>O) and organic compounds like methane (CH<sub>4</sub>), gasoline, diesel and cellulosic biomass. There a number of fuel processing technologies, such as hydrocarbon-reforming, plasma-

reforming and water electrolysis, available to extract hydrogen from contained species. The following paragraphs review these processes and their practicality in automobile application. Hydrocarbon-reforming as the main section of this thesis will be widely described in sections 2.8-2.11.

### 2.4.1 Plasma Reforming

Unlike conventional reforming processes which follow the chemical equilibrium balance. Plasma-reforming processes generate free radicals such as ions and electrons by ionising chemical compounds. This technology is generally classified into thermal (i.e. high temperature plasma) and non-thermal plasma (i.e. low temperature plasma). The former technology required significant thermal energy to overcome the thermal barrier between chemical bonding prior to ionisation. More preferably, latter technology includes methods such as corona, spark, arc and plasma jets that can reduce process energy consumption by promoting free-radicals generation. Its reaction temperature can be as low as room temperature while the excited electron's surface can reach temperature of 10,000 to 100,000K or  $1 \times 10^{-10}$ eV (Petitpasa et al., 2007), this surface reaction makes this technology different from normal chemical equilibrium where complete conversion is typically bound at below 1000°C. A number of authors have reported the potential to produce hydrogen from a number of HC fuels such as, natural gas (Rueangjitt et al., 2009), gasoline (Green et al.,

2000), and diesel fuel (Bromberg et al., 1999). In plasma-catalyst system, (Hoard, 2001) demonstrated that plasma enhanced selective reduction of  $\text{NO}_x$  by improving the oxidation of NO to  $\text{NO}_2$ .

The main drawback of the onboard plasma reforming is the energy supply cannot be easily justified without affecting fuel economy, unless wasted exhaust heat can be recovered into electrical energy. The best process efficiency reported is 79% using arc plasma design; however detail understanding of this process is still not fully explained. Its application onboard a vehicle is therefore impractical as a standalone device, but potentially can be used to aid aftertreatment system performance in reducing emissions.

## 2.4.2 Water-Electrolysis

Water-electrolysis utilises electrical current across electrodes in order to split water into hydrogen and oxygen (R.2.4.2). This process has the advantage of producing extremely high purity hydrogen at a moderate temperature with the absence of a catalyst. The major drawbacks of this technology are the low energy efficiency and the cost dependent electricity input (Schoenung, 2001). Therefore it is currently sufficient only for supplying prototype hydrogen technology at a localised station.

It has been reported by the International Energy Agency (I.E.A.) that the electrical energy required decreases with increase in temperature, even though the overall process

energy input increases slightly (I.E.A., 2006). Providing that free thermal energy is available, the overall electrical energy input can be sustainably reduced. Feasible long term solution has been foreseen by the EU and the US, to utilise the external heat source, such that of high temperature steam from a nuclear reactor or solar thermal energy, can be utilise in conjunction with water-electrolysis process (HFP, 2007). This would allow a potential hydrogen production efficiency of 45 to 50% range to be achieved, compared to approximately 30% for conventional water electrolysis (DOE, 2010).

In terms of using IC engine's exhaust heat as a thermal source, to assist onboard hydrogen production via water electrolysis, the added weight of the water tank required and the overall process energy gain is difficult to be justified.



## 2.5 Hydrogen as Energy Carrier in Transportation

In the automotive application aspect, at atmospheric pressure, low volumetric heating value of hydrogen 11kJ/L, compared to gasoline 31,000kJ/L and diesel 352,000kJ/L presents significant challenges to a hydrogen economy. Technical restrains such as maximum driving range on a single refuel, fuelling station buffer size requirements, and the transportation efficiency between extraction plants and refuelling stations motivate a number of onboard hydrogen storage technologies development such as pressurised gas, cryogenic liquid and

solid state hydrogen in combination with advance materials has shown to have the most potential.

Pressurised hydrogen is the most common industrial storage method up-to-date. It can be compressed and stored in cryonic container up to 700 bars. Similarly, liquification of hydrogen can be pressurised below its freezing temperature, of  $-252.87^{\circ}\text{C}$ , which can hold energy density up to 7 times higher than its gaseous form. The liquification process, however reported, is still about 11 times lower than the density of gasoline, moreover this method is very energy consuming and could consume up to 40% of the energy content of hydrogen (Bossel U. et al., 2004). For these reasons, both of these storages methods are impractical for automobile applications as concluded by (Hua et al., 2011).

Other options such as chemical hydrogen storage technologies claim to offers greater safety and storage capacity and have received considerable interest (DOE: US). This hydrogen storage method works either by an absorptive storage mechanism, where hydrogen is absorbed directly onto the interstices of metals. Or via hydrogen adsorption mechanism, whereas hydrogen is bonded onto highly porous material with maximum surface area such as activated carbon materials. (Sakintuna et al., 2007) concluded that these are still in their early development stage.

An interesting case study by (Wit & Faaji, 2007) assessed a range of onboard storage

technologies with respect to their energetic and economic well-to-wheel performance. In which, they concluded that for the most advanced storage technologies equipped with the best performing PEM-FC hybrid engine up-to-date would provide an energy performance value between 0.1 and 0.2 MJ<sub>p</sub>/km, where gasoline reference is 0.14 MJ<sub>p</sub>/km. It then concluded that even the most advanced hydrogen pathway does not justify enough advantage over fossil or bio-based fuel in order to fulfil a hydrogen economy Table 2-2. Similar conclusion has been drawn by (Edwards et al., 2008), see Figure 2-9. Another government funded research by (W. McDowall and M. Eames, 2007) pointed out that government political frameworks around carbon and climate change is a key uncertainty that affects the vision of hydrogen economy.

**Table 2-2 Hydrogen storage systems overview – taken from (Wit & Faaji, 2007)**

	Pressurised H <sub>2</sub>	Liquid H <sub>2</sub>	Gas on solid adsorbents	Chemical storage	Gasoline	Diesel
Volumetric density (kg.H <sub>2</sub> /m <sup>3</sup> )	23.2-39.4	67.7	62	125	88	134
Gravimetric density (kg.H <sub>2</sub> /kg storage medium)	2-8.5	6-13	10	14	12.6	14
Storage tank weight (kg)	134-29	43-18	High-25	17	-	-
Typical storage temperature (K)	20-69	0.01-2	11.35	6	-	-
Leakage and boil-off (%/day)	273-313	20.3	700	373	-	-
Energy required to free H <sub>2</sub> (MJ/kg H <sub>2</sub> )	-	0.3-0.5	Na	na	-	-
Energy required to free H <sub>2</sub> (MJ/kg H <sub>2</sub> )	-	-	-	17.28	-	-
Well-to-wheel energy performance (MJ <sub>p</sub> /km)					0.14	

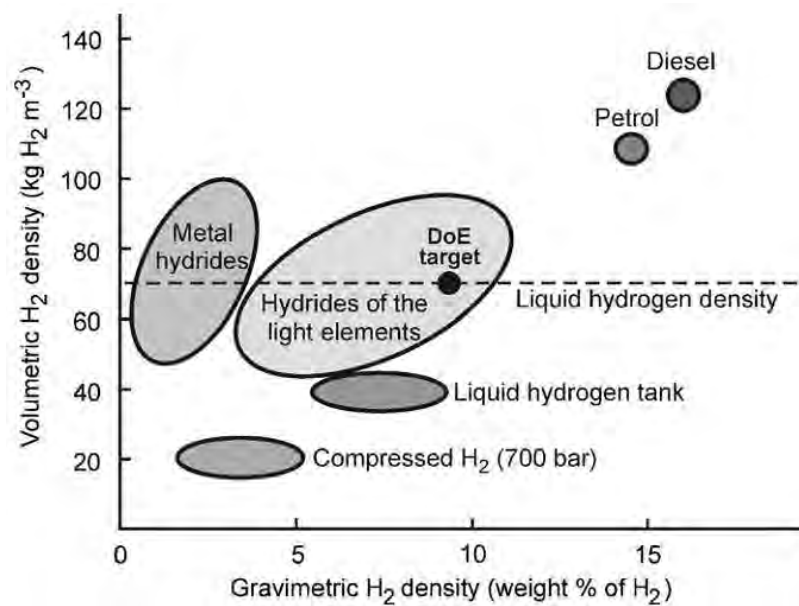


**Figure 2-9 Gravimetric and volumetric densities of various hydrogen storage options (inclusive the wt. and vol. of storage tanks). ‘DoE target’ represents by the US Department of Energy target for hydrogen storage material. (Edwards et al., 2008)**

## 2.6 General Introduction to Catalytic Reforming

Catalytic fuel reforming is a chemical conversion process that separates hydrogen from hydrocarbon containing species, whereby active chemicals coated on a catalyst are employed as reactions enhancers. Reforming reactions can be endothermic or exothermic, and either way does require some sort of energy input to initiate and maintain reaction. This study aims to recover engine exhaust heat as an energy input to promote this reforming process. The potential to use this reformed fuel (gas) as a combustion feedstock is also studied.

## 2.6.1 Exhaust Gas Fuel Reforming

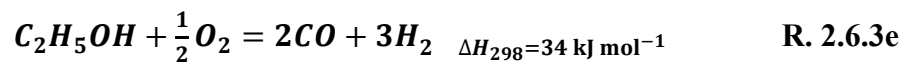
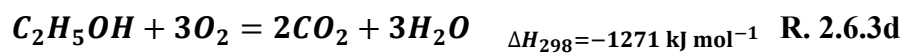
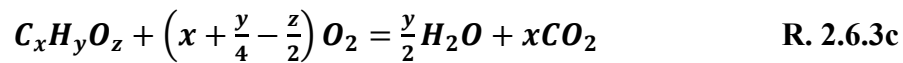
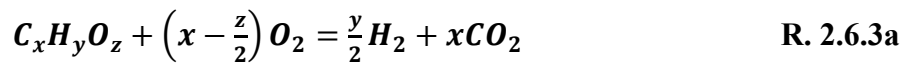
As discussed in section 1.3.2, up to 40% of the fuel input energy is wasted as engine heat rejection. Among the heat recovery technologies, exhaust gas assisted fuel reforming has been extensively studied at the University of Birmingham (e.g. Leung et al., 2009). It is a process which allows hydrogen to be produced onboard a vehicle by retrieving part of the exhaust's heat and waste emissions (i.e. CO, CO<sub>2</sub>, H<sub>2</sub>O and HC) through a catalytic reactor. Whereby primary fuel is injected into the catalytic reformer and reacts endothermically with CO<sub>2</sub> and H<sub>2</sub>O to form H<sub>2</sub> and CO rich reformat. Benefits of this technology include the potential to reduce the size of the aftertreatment system (Sitshebo et al., 2010); improve combustion efficiency and reduce engine emissions by utilising H<sub>2</sub> in the engine as a diesel or gasoline fuel substitute to the engine. This technology can also benefit catalytic after-treatment devices by improving emissions conversion efficiencies and low temperature regenerations ability. Examples of these applications can be found in the studied of (Verhelst & Wallner, 2009); (Nande et al., 2008); (Tsolakis et al., 2004); and (Stishebo et al., 2009). The reforming techniques however vary substantially with combustion modes (i.e. lean combustion of CI and stoichiometric combustion of SI).

## 2.6.2 Main Reaction Paths

The following section gives a brief introduction of the main reforming reactions.

Ethanol is used in their actions in order to provide the reader with a feeling of the theoretical reaction products yield e.g. H<sub>2</sub> and CO<sub>2</sub>, stoichiometric ratios and the net heat of products formation in each reaction.

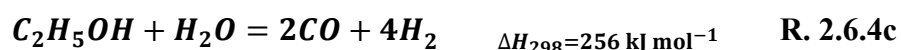
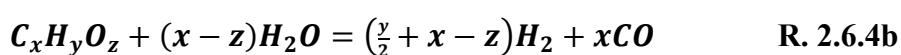
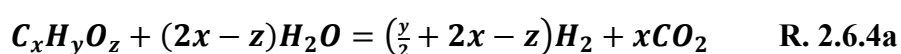
### 2.6.3 Partial Oxidation -POX



POX is a reaction of which oxygen exothermically reacts with hydrocarbon, favoured hydrogen and carbon-monoxide formation. An idealised equation, the oxygen to fuel molecular ratio is very important, it determines) the amount of water molecule required to convert carbon to carbon dioxide or to carbon monoxide, ii) hydrogen yield, iii) hydrogen concentration (mol.%) in product gas, and iv) heat of reaction (Ahmed et al, 1998). Using ethanol - C<sub>2</sub>H<sub>6</sub>O as an example, when O:C ratio = 3, R. 2.6.3 a is a combustion reaction which favoured H<sub>2</sub>O and CO<sub>2</sub> formation, release the highest thermal energy. When O:C ratio = 0.5, R. 2.6.3b is a partial oxidation, which favoured H<sub>2</sub> and CO formation with moderate heat released. Sometimes both reactions can be combined. Though catalytic reformer can

improve the minimum reaction temperature of reactant gas, as an exothermic reaction, POX reaction can be achieved with or without a catalyst. The heat release from such reactions will be carried along the reformer and benefit other temperature dependant reactions (i.e. SRR and DRY).

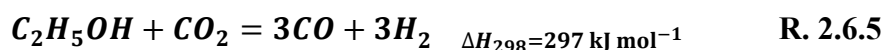
## 2.6.4 Steam Reforming Reaction -SRR



In SRR water react with HC (i.e. fuel) to produce H<sub>2</sub> and CO<sub>2</sub>. The positive heat of reaction indicates a highly endothermic reaction, suggesting that a high temperature is required to maintain efficient reaction, typically >700°C. Likewise, steam to carbon ratio (S:C) is the important factor in this reaction, it determines the amount of steam (i.e. water) molecules required to convert carbon to carbon monoxide or to carbon dioxide. Lower S:C ratios lead to carbon monoxide and hydrogen yield, R. 2.6.12.3a, and a higher S:C ratio leads to the production of carbon dioxide and hydrogen, R. 2.6.1.3b. Using ethanol (C<sub>2</sub>H<sub>5</sub>OH) as example, when S:C ratio = 1, R. 2.6.1.3c has a theoretical hydrogen yield of 67%. Similarly when S:C ratio = 3, R. 2.6.1.3d gives a theoretical hydrogen yield of 75%. Because it is an endothermic reaction, its conversion depends largely on available reactant temperature.

Because the heat of formation is positive, its conversion is largely temperature dependent.

### 2.6.5 Dry Reforming Reaction- DRR



Provided high temperature is available, DRR offers another route to hydrogen production using by-products of fossil fuel combustion as reactants. In which, carbon-dioxide reacts endothermically with fuel to produce carbon monoxide and hydrogen. The higher heat of reaction of DRR than SRR suggests that DRR required a higher temperature input. Using ethanol as an example, a carbon dioxide to carbon ratio C<sub>2</sub>O:C of 1 can yield 50% of carbon monoxide and 50% of hydrogen.

### 2.6.6 Water Gas Shift - WGS



Compared with SRR and DRR, WGS is not as active or H<sub>2</sub> productive due to being thermodynamically inhibited at high temperature. In this reaction carbon monoxide reacts with oxygen molecules, favours carbon dioxide and hydrogen production at temperature below 300°C, R. 2.6.6 (Choi & Stenger, 2003). However, this reaction often serves as a secondary reaction following POX and SRR in an industrial HC reforming plant. The main benefit WGS offers is that, it provides a low temperature route to carbon monoxide purification, and simultaneously increased the hydrogen yield. As carbon monoxide is

considered as a poisoning species in fuel cell catalysts that can deactivate the fuel cell catalyst, WGS is a desired reaction in fuel cell applications.

NB:WGS is undesired when HC reforming is to be used as a combustible gas for two main reasons, i) carbon monoxide is a combustible gas and contain high heat energy than carbon dioxide, and ii) WGS has a lower hydrogen yield than SRR, therefore the consumed water molecule will reduce the overall reforming efficiency.

### 2.6.7 Autothermal Reforming Reaction -ATR

ATR referred as "oxidative steam or dry reforming", it utilises the heat from the exothermic POX to sustain the heat required by the endothermic SRR or DRR, where the ideal net enthalpy of reaction is zero (i.e. thermal neutral). (Kale & Kulkarni, 2010) conducted a dry autothermal reforming experiments under various thermo neutral combinations (i.e. temperatures, pressures and reaction ratios). Of which, they concluded that the maximum hydrogen yield of 2.58 moles, was obtained at reaction temperature approximately 600°C, pressure of 1 bar, CO<sub>2</sub>:C<sub>2</sub>H<sub>5</sub>OH ratio of 1, O<sub>2</sub>:C<sub>2</sub>H<sub>5</sub>OH ratio of 0.5.

(Gallucci et al., 2010) has conducted a theoretical studied of hydrogen production via autothermal reforming of ethanol. He concluded that the heat needed for a complete ethanol conversion can be obtained by burning approximately 15% of the hydrogen recovered from the overall autothermal reforming process.

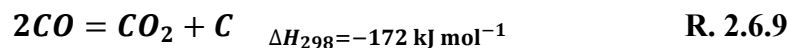
## 2.6.8 HC Decomposition

Depending on the reforming condition, HC fuel can be decomposed into hydrogen and carbon molecules. The fact that this reaction can generate hydrogen that is free from carbon monoxide makes it attractive to fuel cell applications, but it often suffers from poor catalyst life time. (Wang et al., 2008) conducted a methane decomposition experiment; he reported 5 and 22% methane conversion at 700°C with uncoated and Mg-coated catalyst respectively, which is still far from the equilibrium prediction of 83%.

In onboard fuel reforming, the above gives an idea of how a fraction of the HC fuel can be broke down into H<sub>2</sub> and carbon or more likely to be intermediate species (i.e. short chain HC), which reduce the helps the conversion when it entre the catalytic reformer.

## 2.6.9 Boudouard

Boudouard is an undesired reaction in catalytic reforming, where carbon monoxides oxidised forming carbon dioxide and a single carbon molecule. This free carbon or soot often causes coking therefore irreversible effect to catalyst bed.



## 2.7 Benefits of Onboard Exhaust Gas Fuel Reforming

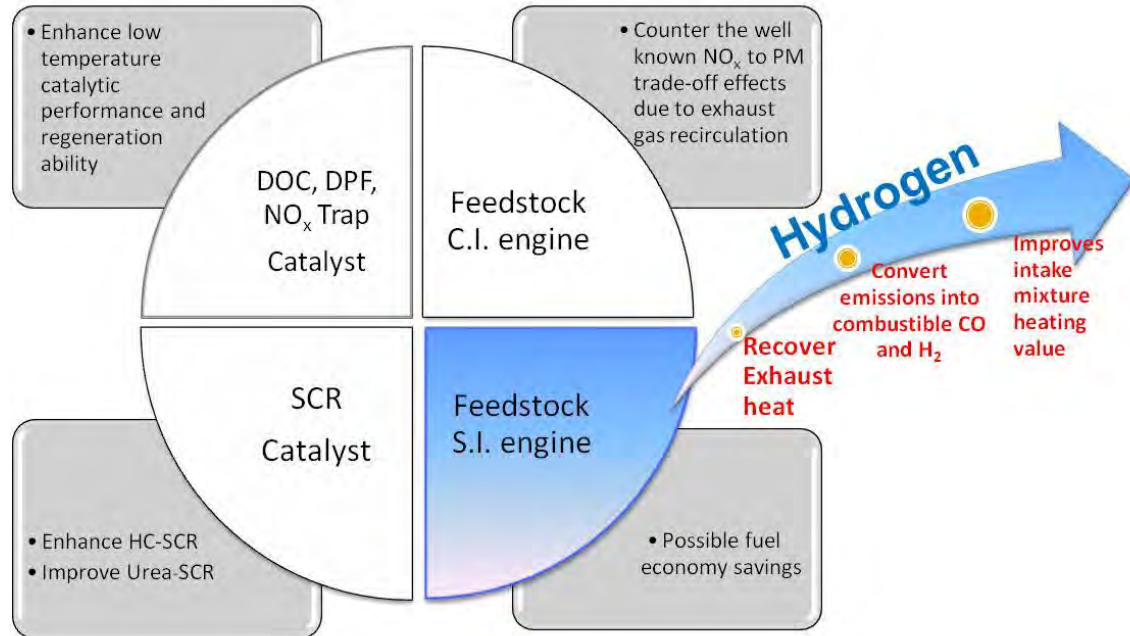


**Figure 2-10 Potential applications of exhaust gas fuel reforming**

The benefits of having hydrogen riched gas on IC engines has been discussed and well researched, an summary of those benefits is illustrated in Figure 2-10.

In aftertreatment for IC engines, (Tsolakis et al., 2004) reported that hydrogen produced from onboard fuel reforming has the potential to improve catalyst activity in reducing emissions or enhance the regeneration process and widen operation window. Meaning there are potentials to reduce the size of after-treatment system or even completely replace some of them, and more importantly there is no necessity for bulky equipment (Sitshebo et al., 2010).

In SI engine applications, it has been reported that adding hydrogen upstream of

TWC helps to further reduce heavy HC species, such as 1, 3 butadiene, which is a cancer related species as reported by (Hasan et al., 2011). (Guo et al., 2005) had concluded that hydrogen addition on SI engine can significantly extend the flammability limit, thus allows leaner premixed flame hence lower CO<sub>2</sub> and NO emissions.

## 2.8 Exhaust Gas Reforming Routes

Exhaust gas fuel reforming is a complex chemical process. If mass and heat transfer are taken out of the equation, the reforming routes can be understood by the following; First of all, the exhaust gas compositions and their concentration (i.e. O<sub>2</sub>, H<sub>2</sub>O and CO<sub>2</sub>) predefine the amount of HC fuel required to achieve individual reaction stoichiometry. By controlling the known amount of HC fuel, the optimum fuel required for maximum production can be achieved. Meanwhile, the overall/net heat of reaction varies, if the overall heat of formation is negative, meaning there is a need of heat supply and vice versa. Options of this heat supply can be coming from i) exhaust gas temperature, ii) POX/ATR via external oxygen and fuel input, iii) electric heat input. Options ii) and iii) often associate with a fuel penalty impact.

For lean exhaust composition produced from CI engines, it contain significant amount of oxygen, carbon dioxide and water. The exhaust temperature is range between 150 to 550°C, which is lower than the typical reforming temperature of SRR and DRR. Therefore

the oxidative DRR and SRR is the preferred route. As a proportion of the injected fuel will be used to supply the heat necessary to rise the reforming temperature, the overall reforming process will have an impact on the overall SFC.

SI engines have a very different exhaust characteristic. First of all, the stoichiometric SI combustion limits the oxygen availability in exhaust. In the contrary, its exhaust gas temperature is significantly higher than that of the CI, it ranges between 550° to 950°C. Retrieving this exhaust heat is a possible option to sustain the overall endothermic reforming reaction without any fuel penalty. In theory, there should be a gain in fuel heating value as the heat energy input is generally considered as a free energy supply.

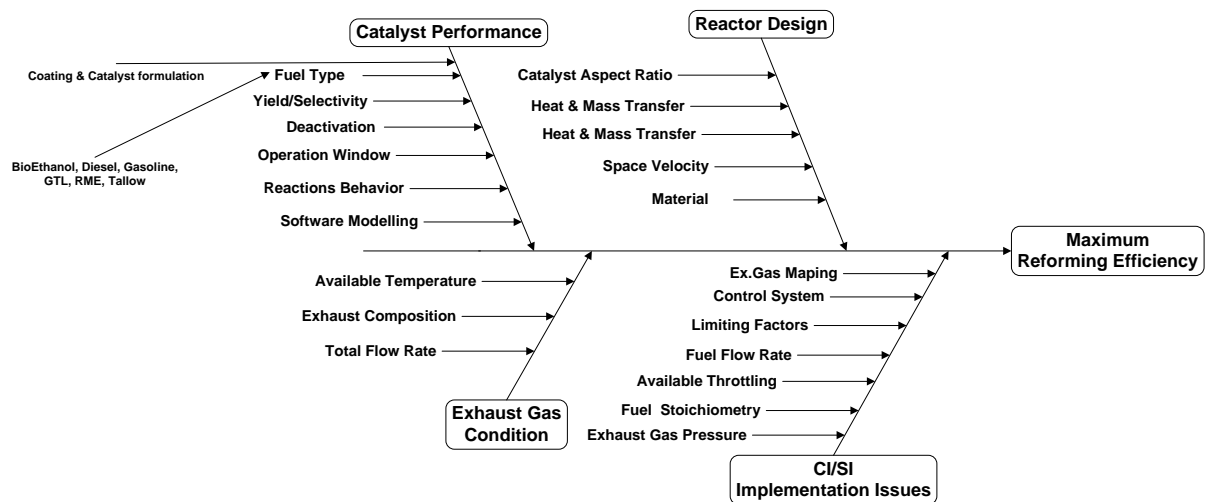


Figure 2-11 Major factors that effects maximum reforming efficiency

To give this project an overview, Figure 2-11 illustrates major factors that could affect the exhaust gas reforming efficiency. It also guides the reader to have a better understanding of the research approach and future works that the author is trying to take.

# CHAPTER 3

## 3 Experimental Setup

This chapter gives details on the equipment used in this study, including reforming test rig and operation conditions. The important data processing techniques and calculations are also described in detail. Please be aware that there are three stages of experiments and testing conditions will be described separately in each chapter.

### 3.1 Reforming Catalyst

A precious-metal reforming catalyst, which was designed for high fuel-conversion and durability, was supplied by Johnson Matthey. It consisted of a high cell-density cordierite substrate (900 cells per square inch) coated in active material of nominal composition 2%Pt-1%Rh (by mass) dispersed on a support containing 30% (by mass) ceria-zirconia (3:1 mole ratio) on 70%  $\gamma$ -alumina. A small core (15mm dia. x 35mm) was cut from the monolith to form the catalyst bed, which was fitted inside a stainless steel reactor that was held vertically within a large tube furnace Figure 3-1. It was a Johnson Matthey proprietary formulation designed to promote all the desired reactions (oxidation, steam reforming, dry reforming, and water gas shift reaction), while at the same time inhibiting coke formation.

### 3.2 Reforming Rig.

The reactor was placed in a tubular furnace and the temperature was controlled by means of a temperature controller. The bed temperature was monitored by K-type thermocouples, one of which (on the catalyst inlet face) was used to set and control each test point, while the other (on the outlet face) was used to check that the product stream temperature was isothermal with the feed stream. The intention was to mimic as closely as possible the anticipated practical design Figure 3 2, in which the reformer is located within the exhaust pipe and surrounded by hot exhaust gas. The other thermocouple that placed inside at the central cell of the monolith was used to record the temperature profile. The arrangement allowed vertical movement of the thermocouple and thus monitoring of the temperature profile. The liquid feed-rate (of HC-fuel and water) was controlled by a medical syringe pump that delivered a fuel into the carrier gas.

After checking that the catalyst activity was stable, its performance was studied at bed temperatures that are likely to be experienced by an exhaust gas reformer when it is close-coupled with an SI engine (G. Stiesch, 2003). The composition of the product stream was analysed at 8 set points between 550° and 900°C (inclusive), allowing the bed temperature to stabilise at each point before the measurements were made.

### 3.3 Exhaust Gas Emissions and Reformate Analysis

Downstream of the reactor, the product gas-stream passed through a condenser and a water trap, before the dry gas was analysed by i) a HORIBA MEXA 7100 analyser to measure CO, CO<sub>2</sub>, THCs and O<sub>2</sub> concentrations (electrochemical method), ii) a HP gas chromatograph equipped with a thermal conductivity detector (TCD) was used for measurement of the H<sub>2</sub> content of the reactor product. A double column arrangement was used; the first column was a 1 m long 1/8 in. diameter Haysep Q, 80–100 mesh and the second a 2 m long 1/8 in. diameter Molesieve 5 A ° (MS5A).

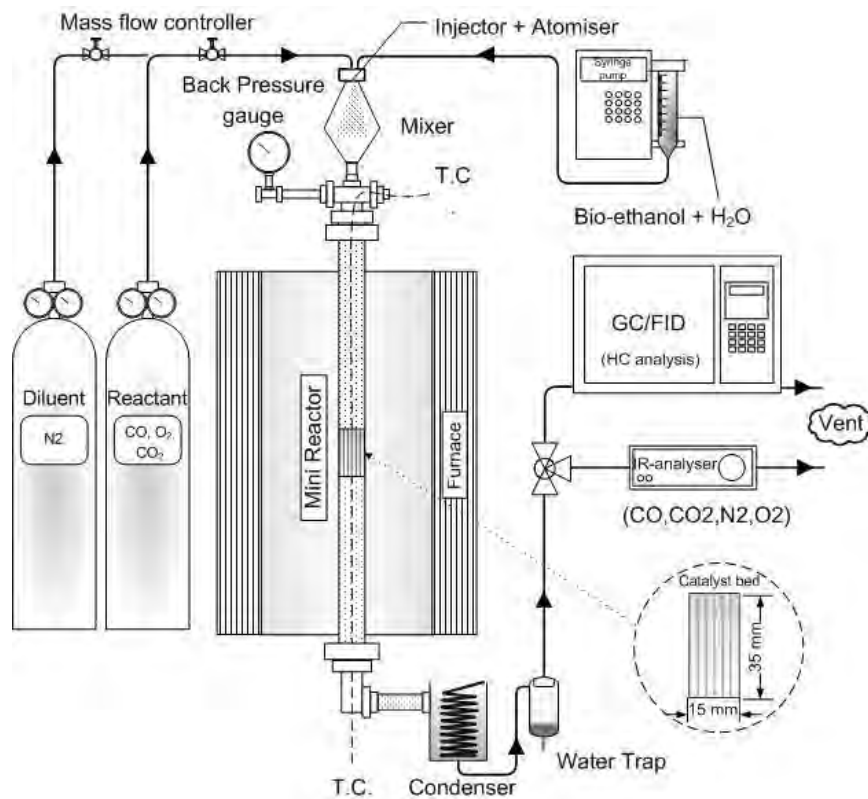


**Figure 3-1 Test equipment for measuring catalyst activity**

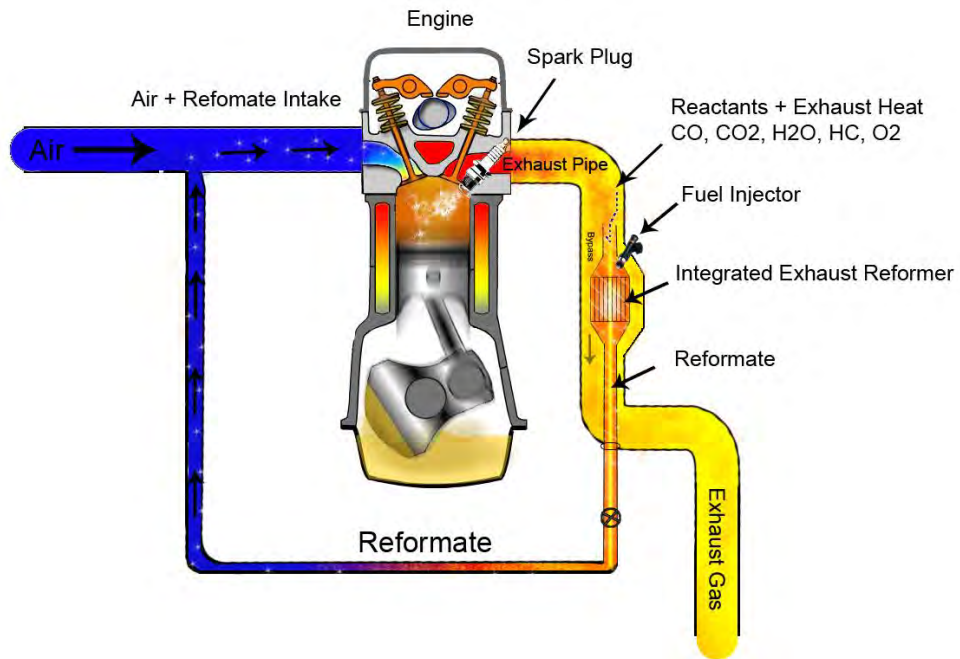


**Figure 3-2 Closed-loop exhaust gas reforming**

### 3.4 Fuel Properties

Fuel grade bioethanol

**Table 3-1 with a purity of 99.7% was supplied by Shell Global Solutions UK.**

**Table 3-1 Bio-ethanol fuel specifications**

Property	Ethanol
Chemical Formula	C <sub>2</sub> H <sub>5</sub> OH
Molecular Weight	46.07
Carbon	52.20%
Hydrogen	13.10%
Oxygen	34.70%
Density, kg/m <sup>3</sup> @ 15.5° C	792
Boiling temperature, °C	77.8
Reid vapour pressure, bar	0.158
Research octane number (RON)	108
Motor octane number (MON)	92
Autoignition temperature, °C	422.8

### 3.5 Calculation

Fuel conversion was calculated from the carbon balance, based on the assumption that all organic species in the product stream were being detected and measured by the gas chromatograph. The gas-hourly space velocity (GHSV; defined in Eq. 3.1) of the feed stream to the catalyst bed was kept at 25,000 h<sup>-1</sup> throughout the ethanol reforming test. The GHSV was based on a design specification for a reforming reactor that would be compact enough to be fitted inside the exhaust system of a passenger car.

$$\text{GHSV (h}^{-1}\text{)} = \frac{1}{\text{Contact time (h)}} = \frac{\text{Catalyst bed volume (m}^3\text{)}}{\text{Feed rate (m}^3\text{h}^{-1}\text{)}} \quad \text{Eq. 3.1}$$

For each component route, the predicted product distribution at chemical equilibrium was calculated using the STANJAN equilibrium model (version 3.89, Stanford University). The calculations were performed for the same reactant stoichiometries and concentrations (at 1 bar; 550° to 900°C) as used in the catalyst tests. The experimental chemical efficiency at each set point was calculated from the molar amounts of H<sub>2</sub> and CO formed, and the C<sub>2</sub>H<sub>5</sub>OH consumed, using their higher heating values (Eq. 3.2). The experimental efficiencies were compared to the maximum value calculated from the reaction stoichiometry for each route.

$$\eta_{\text{Ref}}(\%) = \frac{HHV_{\text{fuelprod}} \dot{m}_{\text{fuelprod}} (\text{CO, H}_2 \text{ and un-reacted CH}_4)}{HHV_{\text{fuelin}} \dot{m}_{\text{fuelin}}} \times 100 \quad \text{Eq. 3.2}$$

### 3.6 Setup for Real Exhaust Gas Fuel Reforming (i.e. chapter 5)

The use of real exhaust gas condition instead of bottle gases requires a slight change in the test rig setup, but the majority of the setup remains the same, see Figure 3.3.

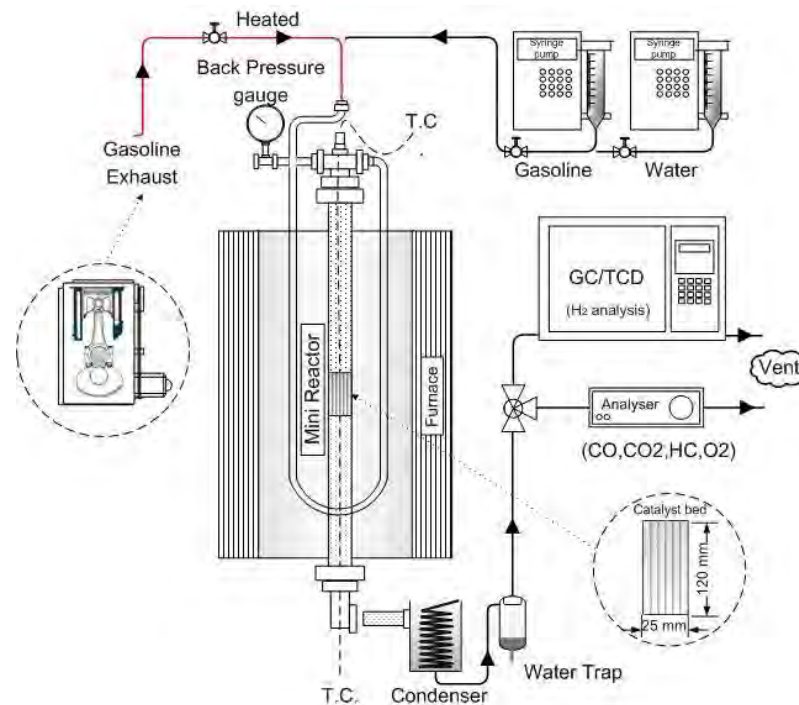


**Figure 3-3 Mini reformer setup**

#### 3.6.1 Engine and Engine Instrumentation:

The experiments were carried out in a naturally aspirated, water-cooled, single cylinder 4-stroke, 4 valves per cylinder, spark-ignition experimental engine. The main engine specifications are shown in Table 3-2.

An electric dynamometer with a motor and a load cell was used to load and motor the engine. The engine test rig included all the standard engine test rig instrumentation to allow monitoring of in-cylinder pressure, flows (fuels, intake air and exhaust gas), temperatures (oil, air, inlet and exhaust manifold) and pressures (gauges mounted at relevant points). Atmospheric conditions (humidity, temperature, pressure) were monitored during the tests.

**Table 3-2 Engine specification**

Bore (mm)	89.9
Stroke (mm)	88.9
Swept Volume (cm <sup>3</sup> )	570.7
Connecting Rod Length(mm)	160.0
Compression Ratio (Geometric)	11.5:1
MBT Spark Timing (BTDC)	24
Fuel Delivery	Port Injection (3bar) and Direct Injection (Optional)
Valves	Intake/Exhaust
Lift (mm)	10.5/10.1

### 3.6.2 Data Acquisitions

Data acquisitions includes the in-cylinder pressure, mass fraction burned (MFB), indicated mean effective pressure (IMEP), percentage of variation (%COV) of IMEP and cylinder peak pressure were recorded by a pressure transducer model kistler 6041A, mounted flush with the cylinder head wall. 300 consecutive cycles were measured with a resolution of

0.5 CAD. Real time measurement of air flow rate was achieved using a Romet G40 rotary gas flow meter, mounted at the air flow inlet before the throttle body, which was connected to a shaft encoder and a tachometer. Flow rate of reformat were controlled by Platonrotameter type flow meters.

### 3.6.3 Fuel Properties

A commercial gasoline fuel supplied by Shell Global Solution Ltd. was used in this study (both engine and reforming fuel). The main fuel properties are shown in Table 3-3.

**Table 3-3 Fuel Properties**

	Standard Gasoline
Chemical Formula	$C_{6.37}H_{11.69}$
Octane No. (RON)	~95
HHV (MJ/kg)	47.0
AFR Stoich.	14.48
H:C ratio	1.835
O:C ratio	0
Enthalpy of Vaporisation (kJ/kg)	~300
Density, $kg/m^3$ @ 15° C	0.7387
IBP (°C)	28.6
FBP (°C)	196.3
Vapour Pressure @20°C (kPa)	~55

# CHAPTER 4

## 4 Catalytic Reforming of Ethanol

This chapter studied the performance and behaviour of separate reforming reaction (i.e. POX, SRR, DRR and WGS) using ethanol as the HC fuel. Utilising ethanol to represent HC-type fuel minimises the amount of complex reactions which may complicate the analysis. This part of the study is important as it provides the fundamental reforming ability/operation windows of the prototype catalyst, hence contributes towards the full feasibility of onboard gasoline exhaust gas reforming. It is worth noting that the heating value of bio-ethanol and gasoline are different, therefore the calculated improve ethanol reforming process efficiency does not apply directly to the gasoline reforming process.

To date, the reforming of bioethanol has largely been studied in the context of hydrogen generation for fuel cell systems (Kolb, 2008). Both base metal and precious metal catalysts have been identified for the reaction with steam (steam reforming) by (Vaidya & Rodrigues, 2006); (Diagne et al., 2002) or with steam and oxygen (oxidative or autothermal reforming) (Klouz et al., 2002), (Deluga et al., 2004). However, the performance of the catalysts depends not just on their activity, but also on their ability to resist deactivation, which can principally occur by

- i) Deposition of carbon-rich species – often caused by dehydration of  $C_2H_5OH$  on the

catalyst surface, followed by cyclisation of the ethene-like species formed as reported in studies (Liguras et al., 2003) and (Breen et al., 2002);

ii) Metal sintering – particularly when high operating temperatures are required (Vaidya & Rodrigues, 2006).

Although base metals have the perceived commercial advantage of being less expensive, they are intrinsically less active for bioethanol reforming than precious metals (Frusteri et al., 2004), and they have to be operated at high steam:carbon ratios (Athanasios, 2004) to avoid carbon deposition. In the context of exhaust gas reforming, precious metals have the additional advantage of requiring neither pre-reduction to induce activity, nor protection from passivation when the reformer is not operational.

We have studied the activity of a bi-metallic precious metal catalysts for the likely H<sub>2</sub>-generating reactions, namely water gas shift, oxidative reforming, steam reforming and dry reforming. (Similar catalysts had previously been shown to be active and durable for exhaust gas reforming of both petroleum-derived hydrocarbon fuels and oxygenated biofuels (Tsolakis et al., 2004). The performance data have allowed us to predict (i) the overall reaction stoichiometry under operating conditions, (ii) the relative contributions from the component reactions, and (iii) the potential benefits of installing this type of reforming technology on board a bioethanol-fuelled vehicle.

## 4.1 Testing Conditions

The experiment conducted at 8 set points between 550° and 900°C (inclusive), to mimic engine operation at different loads. The feed stream to the catalyst bed was kept at 25,000 h<sup>-1</sup> throughout the ethanol reforming test. The composition of the carrier gas was varied, depending on the component route being studied (as listed in Table 4-1 and described in chapter 4.2.2 to 4.2.4.)

**Table 4-1 Potential component reactions in exhaust gas reforming of bioethanol**

<b>R.</b>	<b>Reactions</b>	
<b>1</b>	<b>Complete combustion</b>	$\text{C}_2\text{H}_5\text{OH} + 3\text{O}_2 \rightarrow 2\text{CO}_2 + 3\text{H}_2\text{O}$ $\Delta\text{H}_{298} = -1271 \text{ kJ mol}^{-1}$
<b>2</b>	<b>Steam reforming</b>	$\text{C}_2\text{H}_5\text{OH} + \text{H}_2\text{O} \rightarrow 2\text{CO} + 4\text{H}_2$ $\Delta\text{H}_{298} = 256 \text{ kJ mol}^{-1}$
<b>3</b>	<b>Water gas shift</b>	$\text{CO} + \text{H}_2\text{O} \longleftrightarrow \text{CO}_2 + \text{H}_2$ $\Delta\text{H}_{298} = -41 \text{ kJ mol}^{-1}$
<b>4</b>	<b>Dry reforming</b>	$\text{C}_2\text{H}_5\text{OH} + \text{CO}_2 \rightarrow 3\text{CO} + 3\text{H}_2$ $\Delta\text{H}_{298} = 297 \text{ kJ mol}^{-1}$
<b>5</b>	<b>Partial oxidation</b>	$\text{C}_2\text{H}_5\text{OH} + 1/2\text{O}_2 \rightarrow 2\text{CO} + 3\text{H}_2$ $\Delta\text{H}_{298} = 34 \text{ kJ mol}^{-1}$
<b>6</b>	<b>Dehydrogenation</b>	$\text{C}_2\text{H}_5\text{OH} \rightarrow \text{CH}_3\text{CHO} + \text{H}_2$ $\Delta\text{H}_{298} = 71 \text{ kJ mol}^{-1}$
<b>7</b>	<b>Decomposition of acetaldehyde</b>	$\text{CH}_3\text{CHO} \rightarrow \text{CH}_4 + \text{CO}$ $\Delta\text{H}_{298} = -22 \text{ kJ mol}^{-1}$
<b>8</b>	<b>Boudouard</b>	$2\text{CO} \leftrightarrow \text{CO}_2 + \text{C}$ $\Delta\text{H}_{298} = -172 \text{ kJ mol}^{-1}$

## 4.2 Reforming Testing Procedure

In assessing the significance of our results, we referred to published data for a typical bioethanol-fuelled SI engine operating at around the stoichiometric air:fuel ratio, which show that the main parameter that changes with load is the exhaust-gas temperature (Stiesch, 2003).

### 4.2.1 WGS - Testing Procedure

*Water gas shift:* Water was added at three different rates to a carrier gas of 3% CO in nitrogen (by volume), to produce *steam to CO* (S:CO) ratios of 1.5, 1.0 and 0.5 in the feed stream. In this way, the water gas shift activity of the catalyst could be studied over a range of stoichiometries (from excess H<sub>2</sub>O to excess CO). The CO concentrations were much higher than expected for the exhaust gas (Stiesch, 2003) in order to simulate the generation of reformat in the catalyst bed. The experimental results were compared with predictions from kinetic models (developed using Aspen HYSYS software) based on published data for the homogeneous shift reaction in an uncoated monolith reactor (Bustamante et al., 2004), and with calculations of CO, CO<sub>2</sub> and H<sub>2</sub>O at chemical equilibrium. The kinetic models assumed a plug flow reactor operating at 1bar, where the variables were C:H ratio, flow rate, monolith dimensions, and inlet temperature.

## 4.2.2 SRR - Testing Procedure

*Steam reforming:* Bioethanol was pre-mixed with water in a molar ratio of 1:2, with the stoichiometric excess of H<sub>2</sub>O mimicking the likely situation during exhaust gas reforming. The liquid feed mixture was sprayed at three different rates (30, 60 and 90 ml h<sup>-1</sup>) into a nitrogen carrier gas, the flow of which was adjusted to maintain a GHSV of 25,000 h<sup>-1</sup> to the catalyst bed. In this way, the *steam to fuel* (S:F) ratio and the GHSV were kept constant, while the inlet concentration of bioethanol was varied between 6.8 and 20.3 mol.%.

## 4.2.3 DRR - Testing Procedure

*Dry reforming reaction:* An exhaust concentration of 15 Vol.% of carbon dioxide in nitrogen was used as the carrier gas, to which undiluted bioethanol spray was added at four rates between 28 and 95 ml h<sup>-1</sup>. The CO<sub>2</sub> concentration was close to that typically found in the exhaust from spark ignition engines at most loads (Stiesch, 2003). After adjusting the flow rate of the carrier gas to maintain constant GHSV, the resultant *CO<sub>2</sub> to fuel* (CO<sub>2</sub>:F) ratio in the feed stream was 1.0, 1.5, 2.0 or 2.5.

## 4.2.4 POX - Testing Procedure

*Oxidative Reforming:* In these tests, the ability of the catalyst to oxidise bioethanol to products other than CO<sub>2</sub> and H<sub>2</sub>O was evaluated by using a sub-stoichiometric concentration of O<sub>2</sub> (relative to that required for complete deep-oxidation of the C<sub>2</sub>H<sub>5</sub>OH). A carrier gas

containing 2% oxygen in nitrogen (by volume), representing the worst-case (i.e. highest) O<sub>2</sub> concentration for the exhaust gas, was fed to the catalyst bed at a rate of 3 l min<sup>-1</sup>. Undiluted bioethanol spray was added (at a rate of 8.6 ml h<sup>-1</sup>) to produce an *oxygen to fuel* (O<sub>2</sub>:F) ratio of 0.5 at the standard GHSV. The low absolute O<sub>2</sub>-concentration, effective vaporisation of the bioethanol, and good homogenisation within the mixer prevented any gas-phase combustion taking place upstream of the catalyst bed.

## 4.3 Results and Discussion

### 4.3.1 WGS - Results and Discussion

As most previous studies of bioethanol reforming had been part of the development of fuel processing systems for low-temperature fuel cells (Kolb, 2008), optimising the H<sub>2</sub> concentration in the reformat (to ensure maximum power density) and minimising the CO (which can poison the fuel cell anodes (Palmas et al., 2006)) had been key objectives. The water gas shift reaction, which converts CO and produces H<sub>2</sub>, therefore became an essential component of fuel processing, often carried out in two separate catalytic reactors downstream of the main reformer (Severin et al., 2005). In exhaust gas reforming, however, the shift reaction represents a potential loss in efficiency, by lowering the heating value of the reformat, and generating waste heat rather than consuming it. As a result, the addition of a shift reactor is both unnecessary and detrimental, and even the occurrence of the reaction

within an exhaust gas reformer is undesirable.

The equilibrium constant for the water gas shift reaction declines as a function of temperature as reported by (Satterfield, 1996), which means that the conversion of CO is thermodynamically limited at higher temperatures. At the same time, for a given catalyst, the product distribution generally comes closer to equilibrium as the temperature rises, unless the catalyst is poisoned or thermally/hydrothermally deactivated. In the case of precious metals, (Barbier & Duprez, 1994) reported that Pt-Rh three-way catalysts are known to exhibit high shift-activity during aftertreatment of gasoline exhaust containing a large excess of H<sub>2</sub>O (S:CO = 12.5), at temperatures between 250° and 550°C. Near-equilibrium conversion has also been reported by (Haryanto et al., 2007), of which for a range of ceria-supported platinum group metals at ‘ultrahigh’ temperature (700°C) under biomass gasification conditions where the S:CO ratio was 5.2.

In our experiments, the CO conversion increased almost linearly from 35% at 550°C to 54% at 900°C for all three S:CO ratios (Figure 4-1). The decline in CO concentration was essentially a mirror image of the rise in either H<sub>2</sub> or CO<sub>2</sub> (Figure 4-2), indicating that there was negligible contribution from methanation of either CO or CO<sub>2</sub> (by reaction with H<sub>2</sub> as it formed), as expected from the chemical thermodynamics over this temperature range. This was also confirmed by our gas analysis of the product stream. (We attribute the divergence

between the H<sub>2</sub> and CO<sub>2</sub> traces, particularly at S:CO = 1.5, to the much higher solubility of CO<sub>2</sub> than H<sub>2</sub> in the condensed water during drying of the product stream prior to analysis.) In light of the known shift activity of related catalysts, it was surprising to find that the performance we observed fell short of the chemical equilibrium even at the highest temperatures (Figure 4-3a), but closely matched our kinetic model predictions (Figure 4-3b) that were based on published rate expressions for the forward and reverse shift reactions in a blank monolith (Bustamante et al., 2004). This agreement between the experimental results and the kinetic model indicates that the Pt-Rh catalyst will make a negligible contribution to the shift activity under bioethanol-exhaust conditions, and that any reaction between CO and steam will largely take place in the gas phase.

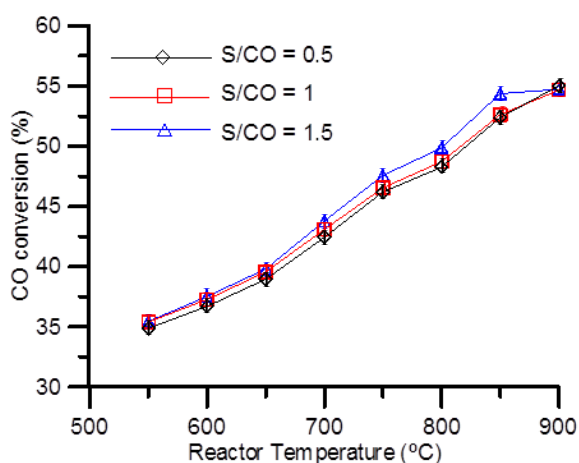


**Figure 4-1 Water gas shift activity as function of temperature: Effect of S:CO ratio on CO conversion.**

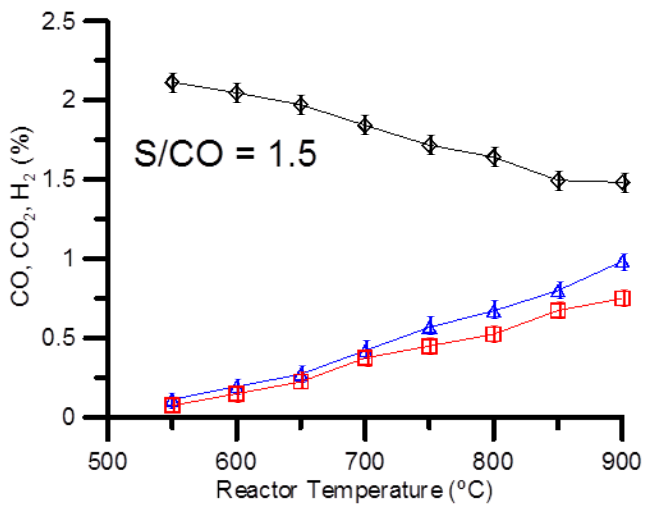
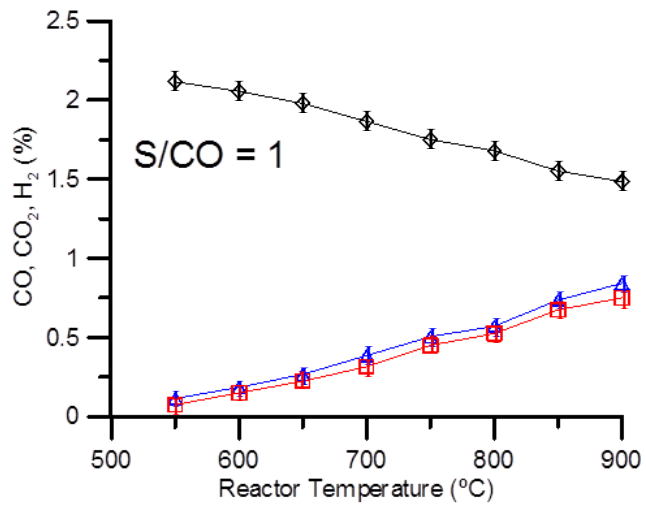
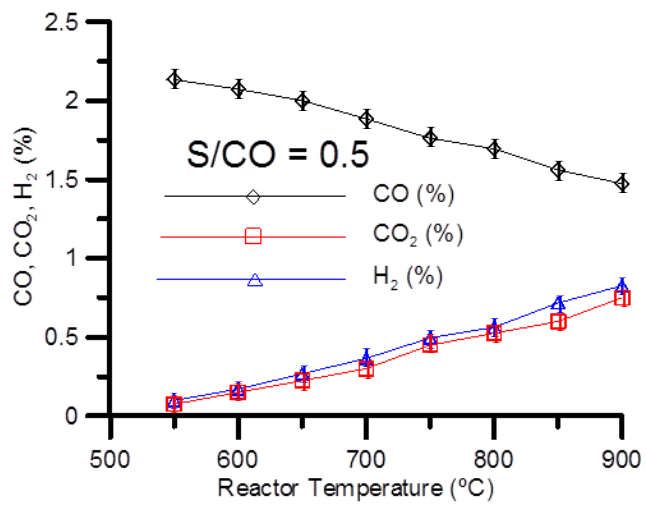


**Figure 4-2 Water gas shift activity as function of temperature: Effect of S:CO ratio on product distribution.**

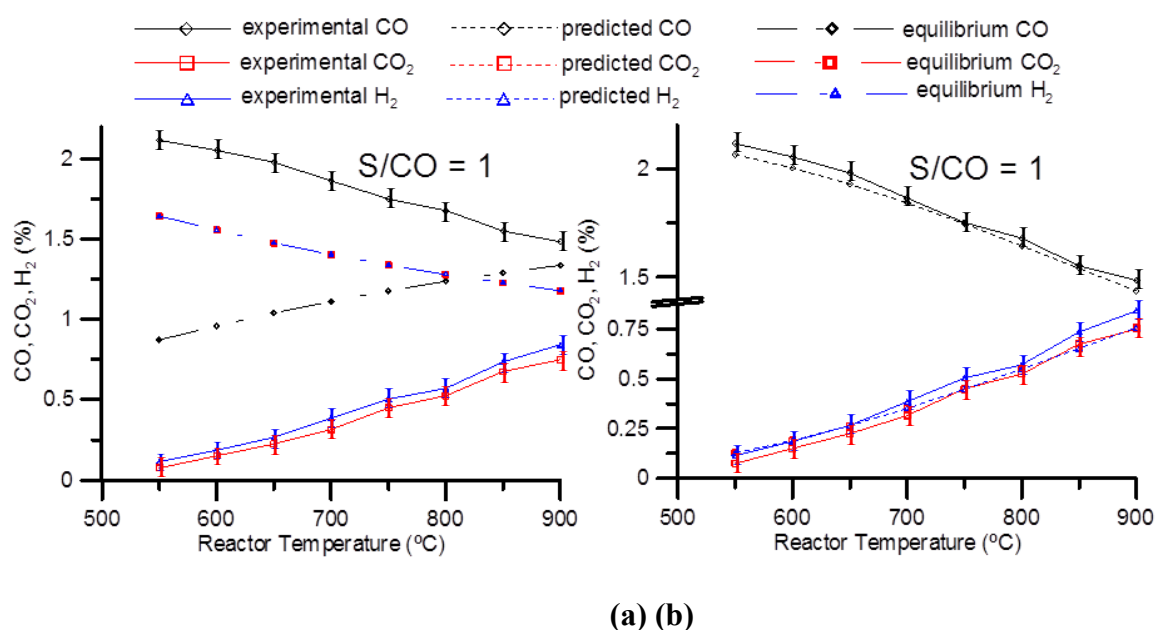


**Figure 4-3 Product distribution during water gas shift testing: (a) Experimental results compared to equilibrium predictions; (b) Experimental results compared to kinetic model prediction.**

### 4.3.2 SRR - Results and Discussion

Our chemical equilibrium models indicated that bioethanol should be completely converted by 650°C under the steam reforming conditions that we used. In practice, although we observed a large step change in activity of the Pt-Rh catalyst between 550° and 600°C, the conversion did not reach 100%; although it came closest at the lowest feed rate, see Figure 4-4. The yield of H<sub>2</sub> showed a similar dependence on temperature and liquid-feed rate see Figure 4-5. This behaviour is consistent with the reaction becoming mass transport limited above 600°C. As one of the features of the catalyst was its high geometric surface area to volume ratio, which was intended to ensure effective mass transfer from the gas phase to the catalyst layer on the monolith, the implication is that intraparticle diffusion was

limiting performance.

As the CO<sub>2</sub> trace in Figure 4-5 confirms, any contribution from the exothermic shift reaction was slight. Close examination of the product distribution at each of the set points showed, however, that the overall reaction was rarely due exclusively to steam reforming, see Table 4-1, R. 2. In fact, the expected product ratio of H<sub>2</sub>:CO = 2 was only observed over a narrow temperature range of 700° to 750°C, see Figure 4 6. Although, from our analysis of the product stream, it is difficult to deconvolute the effects of all the minor reactions of bioethanol, we can tentatively explain some of the deviations from the stoichiometry for steam reforming. Above 600°C, the inflexions in conversion, see Figure 4-4, and in the concentration of unconverted CH-containing species, see Figure 4-5, coincide with the region of highest selectivity to acetaldehyde formation, as reported by (Liguras et al., 2003) under comparable steam-excessive conditions. The occurrence of this reaction, Table 4-1, R.6, would also explain why the H<sub>2</sub>:CO ratio exceeds 2 below 700° to 750°C. At higher temperatures, the immediate decomposition of the acetaldehyde to CO and CH<sub>4</sub>, Table 4-1, R.7, which is known to be an important side reaction during steam reforming on some catalysts as reported by (Kolb, 2008), would account for the recovery in conversion and for the H<sub>2</sub>:CO ratio falling below 2, see Figure 4-6.

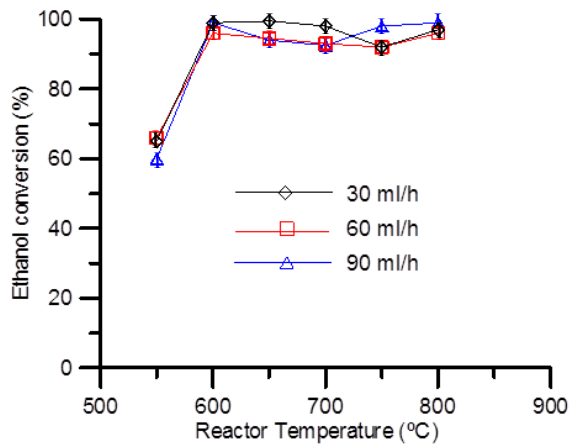


**Figure 4-4 Steam reforming activity as function of temperature: Effect of liquid (bioethanol + water) feed rate on bioethanol conversion.**

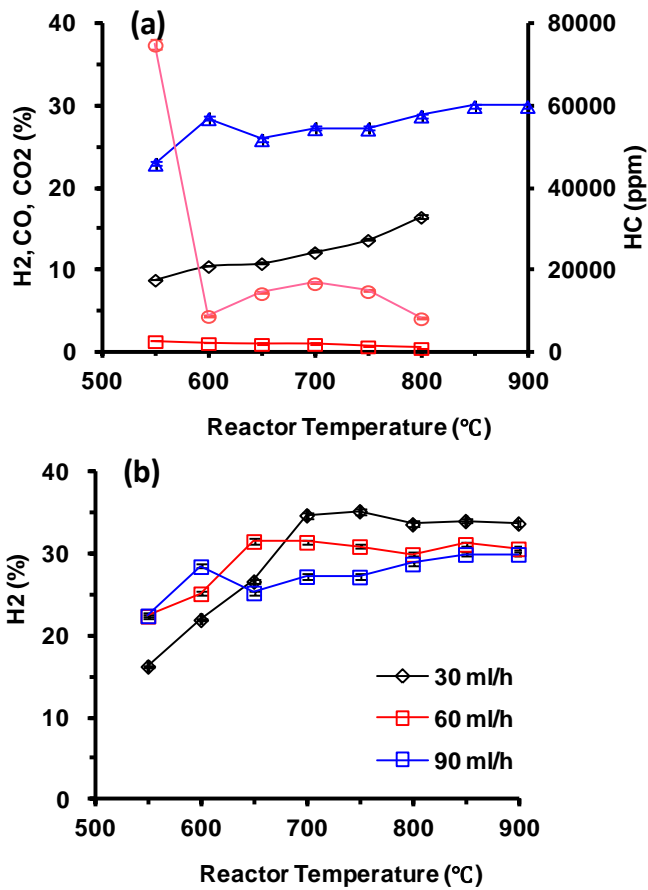


**Figure 4-5 Steam reforming activity as function of temperature: (a) Product distribution at liquid (bioethanol + water) feed rate of 90 ml h<sup>-1</sup>; (b) Hydrogen concentration in product stream at different liquid feed rates. (HC is measure of unconverted or partially converted bioethanol.)**

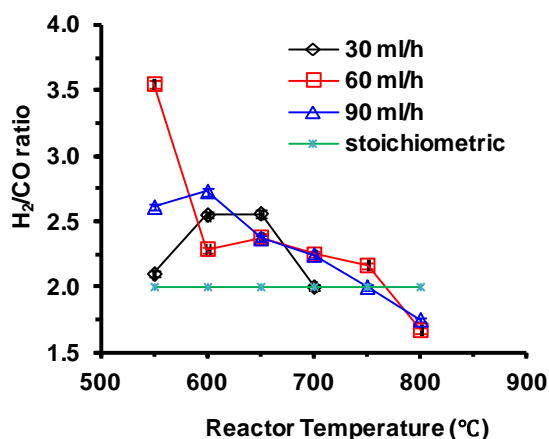


**Figure 4-6 Steam reforming activity as function of temperature: Effect of liquid (bioethanol + water) feed rate on H<sub>2</sub>:CO ratio in product stream.**

### 4.3.3 DRR - Results and Discussion

Unlike the dry reforming of methane, which has been extensively studied by (Hu & Ruckenstein, 2004), there is a scarcity of information relating to the equivalent reaction of ethanol, which is only just beginning to be addressed (Wang & Wang, 2009), (Bellido et al., 2009) and (Hu & Lu, 2009). As the few published results of experimental studies do not relate to comparable conditions or catalyst composition to those we have used to study dry reforming activity under exhaust gas conditions, interpretation of some our data has been made considerably more difficult.

In our tests, the bioethanol conversion rose as a function of temperature below 750°C . The increase gave rise to a smooth curve at the lowest CO<sub>2</sub>:F ratio, whereas a discontinuity occurred between 650° and 700°C at the higher ratios, with a distinct step being apparent at CO<sub>2</sub>:F = 2.5, see Figure 4-7. Below 700°C, there was also a clear correlation between

bioethanol conversion and CO<sub>2</sub>:F ratio, but this did not persist at higher temperatures. These results seem consistent with a high rate of reaction coinciding with a high surface coverage of adsorbed CO<sub>2</sub>, which occurs at the lower temperatures when there is a stoichiometric excess of carbon dioxide in the gas phase. Analysis of the product distribution, Figure 4-8, showed that the H<sub>2</sub>:CO ratio closely matched the expected 1:1 ratio for dry reforming throughout, Table 4-1, R. 4.

At each CO<sub>2</sub>:F ratio, the trace for bioethanol conversion started to plateau above 750°C, before declining between 800° and 850°C, and finally recovering, see Figure 4-7. Overall, the trace resembled the shape seen for catalysts that undergo either a structural change during heating (e.g. Pd-based methane combustion catalysts (Simplicio et al., 2009), or poisoning by a temperature-sensitive species (e.g. sulphur poisoning of three-way catalysts (Ansell et al., 1991)). Although rhodium can detrimentally interact with alumina at high temperatures, our Pt-Rh catalyst was designed to avoid this interaction, which in any case tends to occur under strongly oxidising conditions (Burch et al., 1996). Instead, the high temperature effects are easier to explain by a period of self-poisoning, during which a relatively inert species is formed on the catalyst surface, temporarily blocking some of the active sites. As the thermodynamic models of (Wang & Wang, 2009) show a clear boundary exists between a regime in which carbon deposition is favoured, and one in which the

surface of the catalyst ought to be free of carbon. The position of the boundary lies at around 750° to 800°C at CO<sub>2</sub>:F ratios >1.5, but is displaced to much higher temperatures as the CO<sub>2</sub>:F ratio approaches 1. The inert surface species that formed during our tests is likely to be the carbon-rich product of dehydration and cyclisation of bioethanol as suggested by (Liguras et al., 2003) and (Breen et al., 2002).

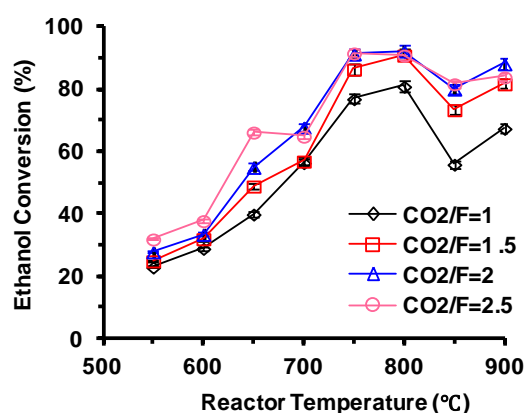


**Figure 4-7 Dry reforming activity as function of temperature: Effect of CO<sub>2</sub>:F ratio on bioethanol conversion.**

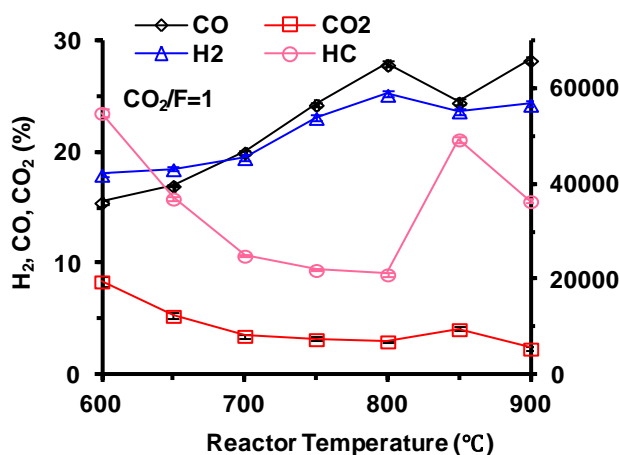


**Figure 4-8 Dry reforming activity as function of temperature: Product distribution. (HC is measure of unconverted or partially converted bioethanol)**

#### 4.3.4 POX - Results and Discussion

Even at the first set-point (550°C) under oxidative conditions, all the oxygen was consumed. However, most of the bioethanol remained unconverted, and very little CO and H<sub>2</sub> was detected Figure 4-9. The conversion was 15%, which is very close to the value predicted (16.7%) for the complete consumption of the available O<sub>2</sub> by catalytic combustion of C<sub>2</sub>H<sub>5</sub>OH (Table 4-1, R. 1).

Above 550°C, the yield of CO and H<sub>2</sub> increased steadily, before levelling above 750°C when the bioethanol conversion reached 100%. The H<sub>2</sub>:CO ratio in the product stream Figure 4-10 revealed two distinct reaction regimes: i) between 600° and 700°C, and ii) above 700°C. The rising proportion of H<sub>2</sub> formed within the low-temperature regime points to an increasing contribution from steam reforming, by reaction of the unconverted bioethanol with the H<sub>2</sub>O generated by catalytic combustion (Table 4-1, R.1). The H<sub>2</sub>:CO ratio peaked at a value close to 2 at 700°C, indicating that the bioethanol was being converted only by combustion and steam reforming at this point. Above 700°C, the H<sub>2</sub>:CO ratio declined simultaneously as the CO<sub>2</sub> concentration, suggesting that dry reforming was now contributing substantially to the conversion of bioethanol. By 900°C, even though several reaction routes were contributing, the H<sub>2</sub>:CO ratio was approaching 1.5, which would be the value expected were all the bioethanol being converted by direct partial oxidation

(Table 4-1, R.5).

Although from the product-distribution trends, it is tempting to envisage that catalytic combustion (producing  $\text{CO}_2$  and  $\text{H}_2\text{O}$ ), steam reforming (consuming the  $\text{H}_2\text{O}$  formed) and dry reforming (consuming the  $\text{CO}_2$  formed) took place consecutively both in the catalyst bed and as a function of temperature, there was clearly some overlap, particularly between steam- and dry-reforming. As comparison of Figure 4-4 and Figure 4-7, both reactions could occur over the entire temperature range, but the rate of steam-reforming was consistently higher. From Figure 4-9, it can be seen that by  $600^\circ\text{C}$  the conversion of  $\text{C}_2\text{H}_5\text{OH}$  had exceeded 67% (the value predicted for the sum of catalytic combustion and steam reforming; Table 4-1, R.1 + R.2), but the  $\text{H}_2:\text{CO}$  ratio in the product stream did not reach the expected value of 2 until  $700^\circ\text{C}$ , Figure 4-10. These results indicate competition at the lower temperatures, with steam-reforming increasingly dominating as a function of temperature, until all the  $\text{H}_2\text{O}$  produced by catalytic combustion has been depleted ( $>700^\circ\text{C}$ ). Under exhaust gas reforming conditions, of course, steam-reforming would not be limited by the availability of  $\text{H}_2\text{O}$  at the highest temperatures, and would therefore be expected to continue to be the predominant endothermic reaction.

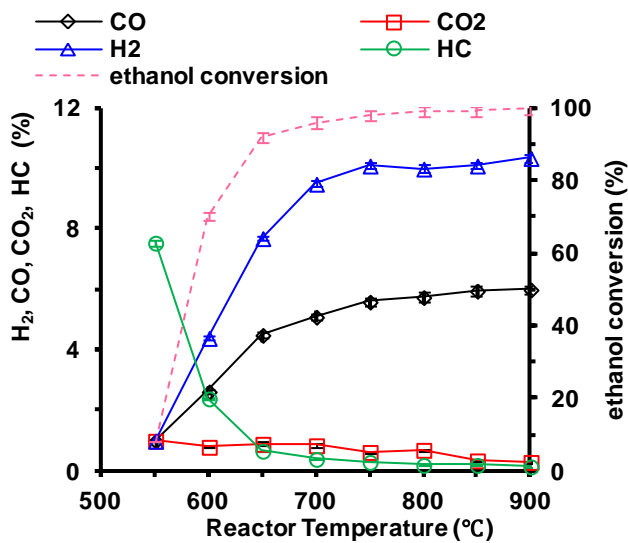


**Figure 4-9 Oxidative reforming activity as function of temperature: Product distribution. (HC is measure of unconverted or partially converted bioethanol.)**

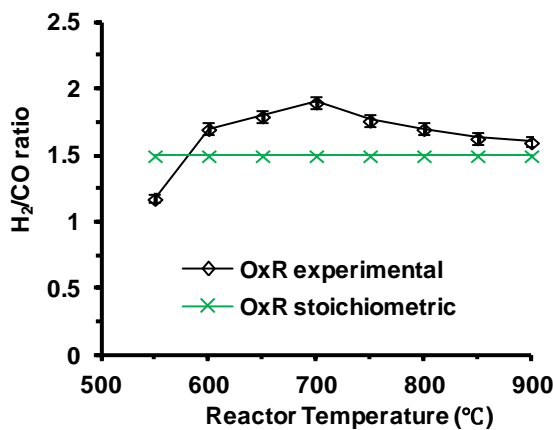


**Figure 4-10 Oxidative reforming activity as function of temperature: H<sub>2</sub>:CO ratio in product stream compared to ratio predicted from reaction stoichiometry.**

### 4.3.5 Chemical Efficiency

The composition of the product stream for each component route and at each set-point allowed us to track the changes in chemical efficiency, which in effect is a measure of both heat recovery and relative fuel heating value. An efficiency value >100% indicates that the process is net endothermic, and that the reformate produced will have a higher heating

value than the bioethanol consumed. For each of the three routes, the chemical efficiency increased steeply as a function of temperature, before stabilising above 700°C, see Figure 4-11. The ranking at most set-points was: steam reforming > dry reforming > oxidative reforming. The maximum efficiency that we achieved during the tests exceeded 100% for each route, but the theoretical maximum was only reached in the case of oxidative reforming (106%).

As our results indicate that oxidative reforming over the Pt-Rh catalyst is a combination of combustion and the endothermic reforming reactions, we expect the instantaneous efficiency during exhaust gas reforming to reflect the balance between these reactions. In particular, if the oxygen concentration in the exhaust gas is below the worst-case value (2%) that we have used in our tests (which seems probable), the effect will be to limit catalytic combustion, allowing a greater proportion of the bioethanol to be converted by the more efficient heat-recovering reactions. We anticipate that a hot (>700°C) exhaust gas low in oxygen will provide the optimum conditions for efficient conversion of bioethanol. With steam reforming being the dominant reaction, the efficiency should approach 120%, meaning that the reformat would have 20% higher fuel heating value than the bioethanol consumed.

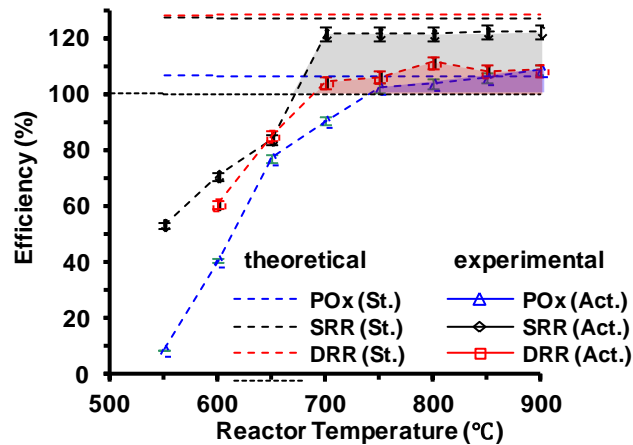


**Figure 4-11 Measured and theoretical efficiencies of reforming routes as functions of temperature. (SSR: steam reforming reaction; DRR: dry reforming reaction; OxR: oxidative reforming.) Shading shows when heat recovery will take place.**

#### 4.3.6 Implications for Fuel Economy

Up to present, it can be concluded that the chemical efficiency is very sensitive to temperature, in a practical system the reformer should be close-coupled with the engine, so that there is minimal heat loss from the exhaust gas before it reaches the catalyst bed. Assuming that a bed temperature of around 750°C can be achieved and maintained, the fuel heating value of the reformat produced should be at least 5% higher than that of the bioethanol consumed by the reformer. By comparison, oxidative reforming of a conventional hydrocarbon fuel or RME produces reformat with a substantially lower fuel heating value than that of the feed, as report in (Elghawi et al., 2008) study. The efficiency with which the bioethanol is converted in the reformer will rise during those parts of the engine cycle that produce a hotter exhaust gas or a lower concentration of O<sub>2</sub>. For a fixed feed-rate to the

reformer, the effect of a lower O<sub>2</sub> concentration will be to shift the balance from combustion to steam- and dry-reforming in the catalyst bed, while a higher temperature will allow steam reforming to dominate.

Feeding the reformat back to the engine will clearly have the direct effect of raising the calorific value of the fuel. If a reformer improves the fuel heating value by 5 to 20% while consuming 40% of the total bioethanol feed, this should translate into a 2 to 8% increase in the fuel economy by heating value solely. Furthermore, (Ji & Wang, 2009) reported as the adiabatic flame speed of hydrogen ( $237\text{cm s}^{-1}$ ) is five times faster than that of gasoline-type fuels ( $42\text{cm s}^{-1}$ ), its addition will improve the thermal efficiency and operating stability of the engine, potentially increasing the fuel economy by a further 10 to 15%. The improvement in combustion is also expected to have a beneficial impact on specific emissions, particularly on NO<sub>x</sub> and VOCs as reported by (Anderson, 2009) study, but these expected benefits are difficult to quantify on the basis of our current knowledge.

It is also worth stressing that exhaust gas reforming is known to promote other forms of internal combustion, such as diesel and homogeneous charge compression ignition (HCCI) (Yao et al., 2009), which are intrinsically more efficient than SI. In the case of HCCI, it has been demonstrated by (Mack et al., 2009) that stable combustion can be achieved with a fuel containing 60% bioethanol and 40% water, which would already substantially reduce the en-

ergy required during processing of the raw bioethanol (typically containing 65% water). If by adding an exhaust gas reformer, hydrated bioethanol with >40% water could be used to fuel mobile and stationary engines, there would be a further beneficial impact on the overall energy cycle. Currently, about 30% of the total energy consumed in the manufacture and supply of hydrous bioethanol is accounted for by distillation, with a further 20% required to make the anhydrous fuel, reported by (J. H. Mack et al., 2009).

#### 4.4 Chapter 4 Conclusions

We have shown that a Pt-Rh catalyst is active for most of the reaction routes expected during exhaust gas reforming of bioethanol with the exception of the water gas shift reaction, which occurs mainly in the gas phase. In our most representative tests, a series of consecutive (but interdependent) reactions took place, starting with catalytic combustion. The H<sub>2</sub>O and CO<sub>2</sub> produced were subsequently consumed during steam- and dry-reforming of the remaining bioethanol. In an exhaust, where there will be a continuous source of excess H<sub>2</sub>O and CO<sub>2</sub>, steam-reforming is expected to be the dominant endothermic reaction. Based on a worst case scenario, in which the exhaust gas contains 2% O<sub>2</sub>, heat recovery will start at 750°C, even though a proportion of the bioethanol will be converted by catalytic combustion in the reformer. In the absence of O<sub>2</sub>, the threshold for heat recovery is predicted to be 50° to 100°C lower. The recovered heat will be in the form of chemical energy that can be recycled

to the engine.

# CHAPTER 5

## 5 Actual Exhaust Gas Reforming

### 5.1 Investigation into the Feasibility of Actual Exhaust Gas Reforming

Following the studies of the previous chapter, the performance of the catalytic reformer is investigated under actual exhaust gas conditions, with both the engine and the reformer fuelled with gasoline fuel. As the reformer is exposed to actual exhaust gas the potential of catalysts coking or deactivation, a more realistic fuel saving at various exhaust gas temperature (600° to 950°C) can be estimated from this setup. Experiment is conducted in a fixed exhaust gas condition with varying furnace temperature between 600° to 950°C.

### 5.2 Reforming Conditions

The reforming experimental conditions are shown in Table 5-1. The study was mainly concentrated on the reactor performance under a range of exhaust gas temperature (600° to 950°C) to mimic engine operation at different loads. The fuel flow rate was adjusted based on the engine exhaust gas composition, intended to match the equivalent stoichiometric conditions of SRR, DRR and POX reactions. The small changes in space velocity were ignored as it was approximately constant. The main reforming reactions of gasoline are presented in

Table 5-2.

**Table 5-1 Engine exhaust gas composition and reforming conditions**

Exhaust gas composition					
CO	CO <sub>2</sub>	O <sub>2</sub>	H <sub>2</sub> O	THC	NO <sub>x</sub>
0.28 %	13.1%	2.4%	12.48%	5224ppm	1885ppm
Reforming conditions					
Temp.	Ex.gas	GHSV	Overall O:C (Excl. H <sub>2</sub> O)	S:C	Fuel flow
600-950°C	3L/min	2000hr <sup>-1</sup>	0.07	0.69	37.2ml/h

**Table 5-2 Reforming reactions of gasoline**

$C_nH_{1.835n} + 1.459nO_2 \rightarrow nCO_2 + 0.918nH_2O$	COX	R.5.2a
$C_nH_{1.835n} + 0.5nO_2 \rightarrow nCO + 0.9175nH_2$	POX	R.5.2b
$C_nH_{1.835n} + nH_2O \rightarrow nCO + 1.918nH_2$	SRR	R.5.2c
$C_nH_{1.835n} + nCO_2 \rightarrow 2nCO + 1.835nH_2$	DRR	R.5.2d
$CO + H_2O \rightarrow CO_2 + H_2$	R/WGS	R.5.2e

## 5.3 Results and Discussion

### 5.3.1 Reformer Products

Hydrogen and carbon monoxide concentrations rose as a function of temperature, along with a decline in CO<sub>2</sub> Figure 5 1. A trend that indicates that the exhaust gas reforming of gasoline is an overall endothermic reforming process. This is a result of the combined SRR and DRR reactions (Tomishige et al., 2004). Fuel reforming in the absent of oxygen, it is likely to also form intermediate HC species by thermal cracking of the gasoline fuel.

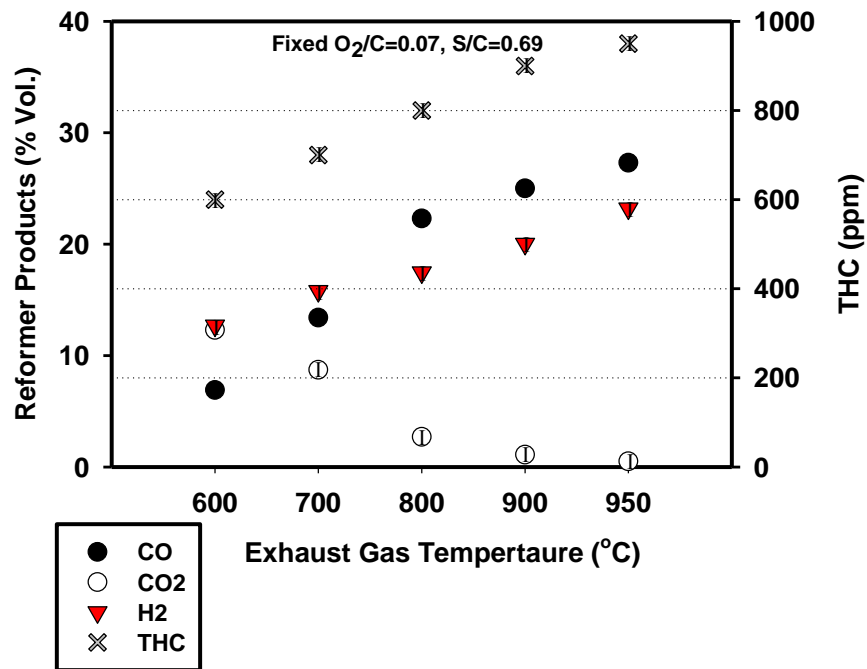


**Figure 5-1 Effects of exhaust gas temperatures on reforming products**

The CO trace follows a sharp rise between the temperature regimes of 600° and 800°C, and continues to rise with respect to temperature at a reduced rate. However the H<sub>2</sub> trace follows a linear rise throughout the temperature test points. As a result, two distinctive H<sub>2</sub>:CO ratios of 1.84 and 0.83 are observed, separating at the temperature of 750°C. These results coincided with the expected stoichiometric ratios of SRR and DRR reactions, H<sub>2</sub>:CO of 1.92 and 0.92, respectively. Suggesting the reforming process is mainly dominated by SRR reaction at exhaust gas temperatures regime below 750°C, and DRR reaction for temperature above 750°C. Furthermore, in chapter 4 we have suggested that SRR and DRR reactions become active at temperature regimes near 650° and 750°C, respectively, which coincided with the above scenario as reported by (Mei, 1979). At exhaust gas temperatures

of 950°C, approximately 23% of the H<sub>2</sub> trace was achieved under gasoline exhaust gas reforming at S:C ratios of 0.69.

### 5.3.2 Reformer Temperature Profiles

From the temperature profiles along the catalyst bed shown in Figure 5-2, it can be seen that at 600°C exhaust gas temperature, there was approximately a 30°C rise in the reaction temperature within the first few centimetres due to the exothermic reactions. It is in accordance with the reactor product, suggesting that the oxygen content (approximately 2%) in the engine exhaust steam is still incapable of generating enough heat that steam and dry reforming reactions required via partial oxidation. Beyond the oxidation zone (i.e. after the first few centimetres from the catalyst bed inlet) the relatively linear drop in reactor temperature suggests that the endothermic SRR and DRR were not very active. The decline in the reactor temperature may also be a result of the thermal cracking of the fuel. This is in agreement with the HC speciation trends, where the most of the un-reacted HCs remained as heavy species, e.g. benzene. At higher exhaust gas temperatures of 800° and 900°C, the highly endothermic reactions of SRR and DRR caused a sharp reduction in the reaction temperatures at the first few centimetres of the catalyst inlet. Furthermore, the reduction at the exhaust gas inlet temperature of 900°C is less significant compared to exhaust gas inlet temperature of 800°C. This suggests that at 800°C, the thermal energy supplied by the

exhaust gas was approximately balanced with the energy required by the majority of the reforming processes.

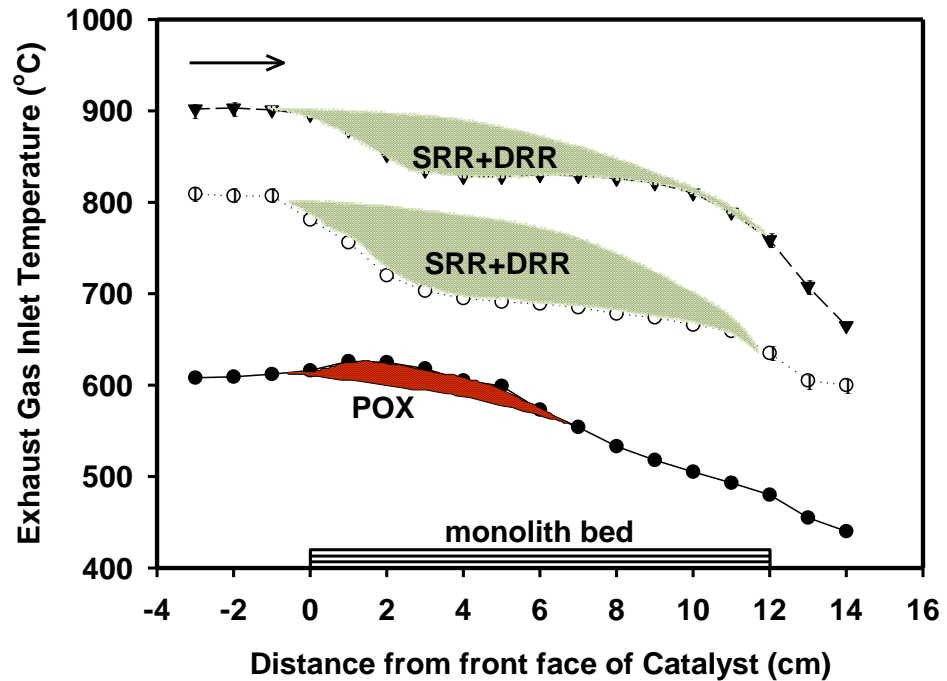


Figure 5-2 Temperature profiles along catalyst bed

### 5.3.3 Process Efficiency

During the closed coupled gasoline exhaust gas reforming process, the combined syn-gas (i.e. H<sub>2</sub>, CO and un-reacted HC) will be fed to the engine inlet as a whole. Therefore the calculation of the reformer fuel efficiency includes the heating energy contained in the un-reacted HC, in contrast to the calculations of the process efficiency where only H<sub>2</sub> or H<sub>2</sub> + CO are included. Resulting in enhanced energy content between 107 to 119%, see Figure 5-3.

$$\eta_{\text{ExhGas Ref}}(\%) = \frac{HHV_{\text{fuelprod}} \dot{m}_{\text{fuelprod}}(\text{CO, H}_2 \text{ and un-reacted CH}_4)}{HHV_{\text{fuelin}} \dot{m}_{\text{fuelin}}} \cdot 100 \text{ Eq.5.1}$$

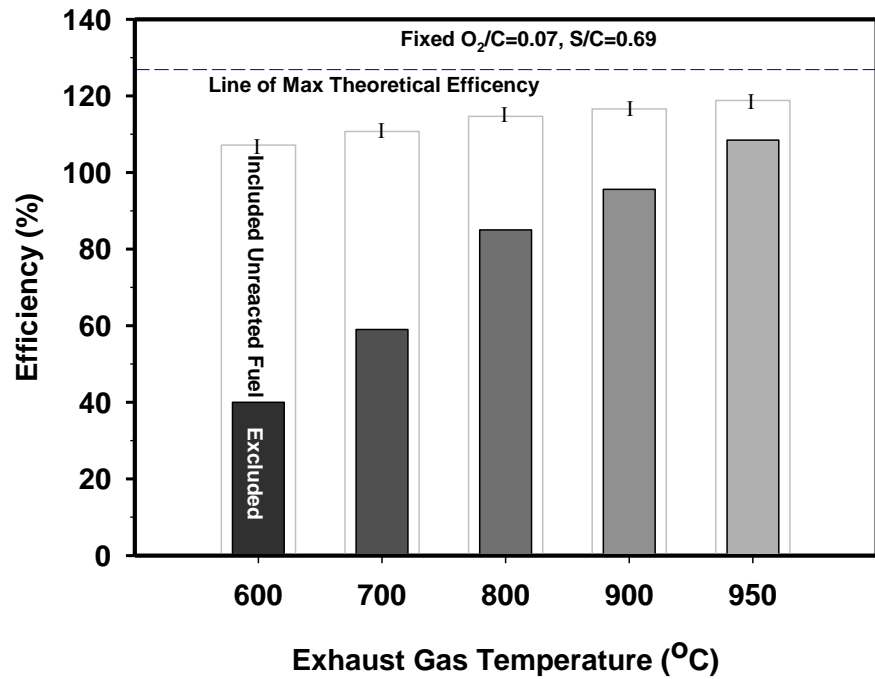


Figure 5-3 Effects of exhaust gas temperatures on reforming efficiency

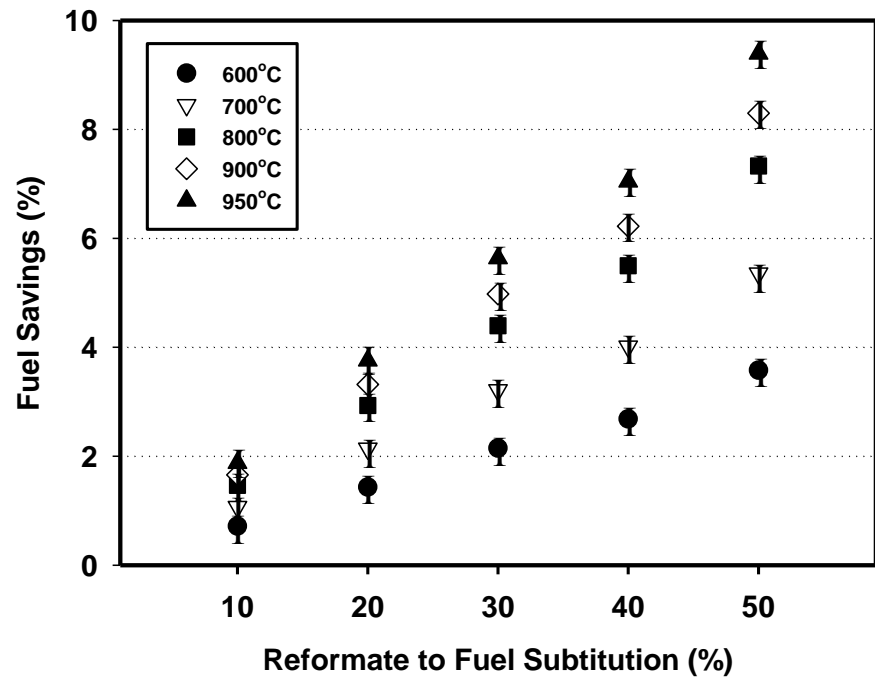


Figure 5-4 Effects of amount of reformate against estimate fuel saving based on current reactor results.

It is estimated that if 10 to 50% of the gasoline fuel is being replaced by reformate, a

potential fuel saving of 3.6 to 9.4% is feasible, see Figure 5-4. These promising results are mainly contributed to the recovery of wasted exhaust heat which initiates the endothermic reforming reactions.

Furthermore, the close-coupled reforming requires a wider engine throttle opening position, in order to maintain the stoichiometry of combustion. This widened throttle will result in reduced engine pumping losses and is likely to provide additional fuel savings of approximately 1 to 2%.

## 5.4 Chapter 5 Conclusion

In this study the reforming catalyst performance was investigated under real gasoline exhaust gas fuel reforming conditions, with varying exhaust gas temperatures. The reforming catalyst showed no sign of deactivation or coking. Based on the examined exhaust gas temperatures (600° to 950°C), a realistic approximation of 3.6 to 9.4% fuel saving are estimated when the engine is closed-couple with exhaust gas fuel reformer. The gasoline exhaust gas fuel reforming efficiency mainly relies upon the exhaust gas temperatures. It is known that in an overall endothermic reaction, by adjusting the GHSV (e.g. by reducing the gas flow rate via the catalyst or increasing the catalyst volume/loading would be beneficial for the reaction conversion, therefore further optimisation could be achieved even higher

reforming efficiency or maintain the same reforming conversion at a lower exhaust gas temperature.

These fuel savings can further be improved when pumping losses from the more favourable engine throttle operation are taken into account, this will be discussed in the next chapter.

# CHAPTER 6

## 6 Partial Gasoline Replacement by Simulated Reformate

### 6.1 The Effect of Simulated Reformate (CO + H<sub>2</sub>) as Fuel Replacement on Engine Performance

In this chapter, a proportion of the engine fuel is replaced with simulated reformate (CO + H<sub>2</sub>). The reformate composition is selected based on the actual exhaust gas reforming performance at exhaust gas condition of 800°C from chapter 5. This will allow i) the combustion performance and ii) actual fuel saving to be studied under the influence of reformate as a fuel replacement.

### 6.2 Reformate Properties

The simulated reformate composition, used in the combustion studies was selected based on gasoline exhaust gas reforming experiments using a mini catalytic reformer, which conducted under the same engine operating conditions, see Table 6-1,. Therefore the reformer conversion efficiency under the current reactor setup and exhaust gas limitation were taken into consideration.

**Table 6-1 Simulate reformat composition**

CO	HC	CO <sub>2</sub>	O <sub>2</sub>	H <sub>2</sub>	H <sub>2</sub> O	N <sub>2</sub>
%	ppm	%	%	%	(%)	%
22.3	12500	2.7	0	17.46	0	56.3

### 6.3 Testing Procedure and Conditions

The engine was warmed up at low load until the oil and water reached its operating temperatures of  $85^{\circ}\pm 5^{\circ}\text{C}$  and  $95^{\circ}\pm 3^{\circ}\text{C}$ , respectively before carried out any experiment. All readings (e.g. emissions) are an average of minimum two readings on at least two separate occasions. A minimum of 5 mins was allowed before any reading was taken for the engine stabilisation. Throughout the experiments the engine was operated at a fixed engine condition with three different reformat flow rates of 15, 20 and 25 L/min, progressively replace 18, 23.9 and 29.9% of the gasoline fuel by mass. Before any results were concluded, fuel pulse width, throttle position and MTB timing was adjusted accordingly to match the IMEP of baseline condition, whereby the combustion analysis and fuel saving (see Eq. 6.3 for calculation) were recorded. Table 6-2 shows the experimental conditions. See Figure 6-1 for the experiment measurement flowchart. The fuel supply system for standard gasoline and reformat is demonstrated in Figure 6-2.

**Table 6-2 Experimental Conditions**

Conditions	Engine Speed	IMEP	Ex. Gas Flow	Engine Fuel Flow	Reformate to Engine Flow	Fuel Required by Reformer	Equivalent Engine Fuel Replacement	Expected fuel saving for 100% conversion	Expected fuel saving for reactor performance at 800°C
	rpm	bar	L/min	ml/h	L/min	ml/h	%	%	%
Baseline	1500	2.34	128.11	918.48	0	Na	Na	Na	Na
1	1500	2.34			15	159.7	18.0	5.91	3.29
2	1500	2.34			20	212.5	23.9	7.53	4.37
3	1500	2.34			25	265.6	29.9	9.16	5.47

$$FuelSaving(\%) = \left(1 - \frac{\dot{m}_{fuel_{Engine_{new}}} + \dot{m}_{fuel_{Reformer}}}{\dot{m}_{fuel_{Engine_{Baseline}}}}\right) \times 100 \quad Eq. 6.3$$

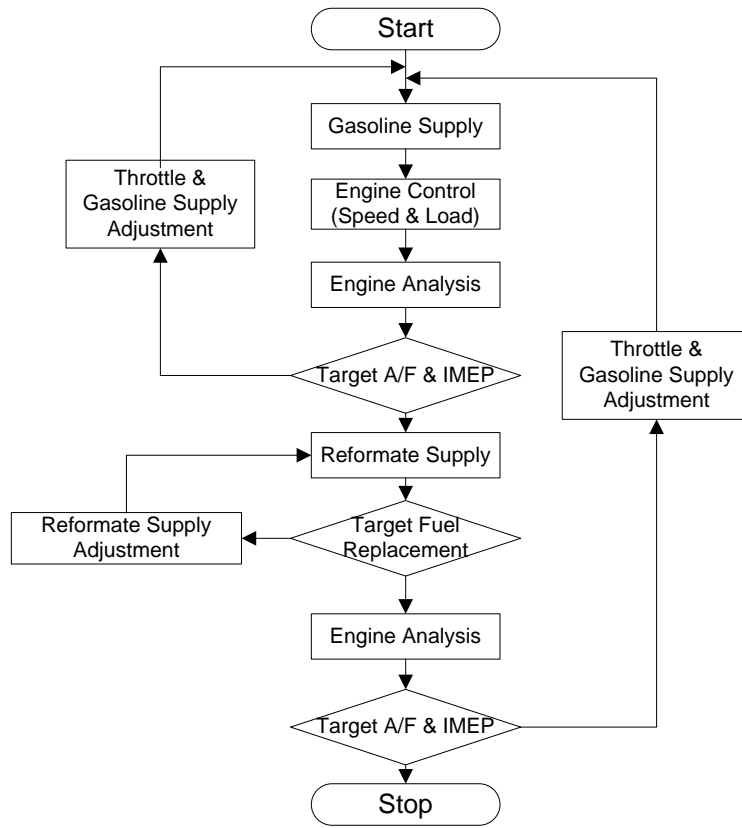


**Figure 6-1 Flowchart of experiment measurement**

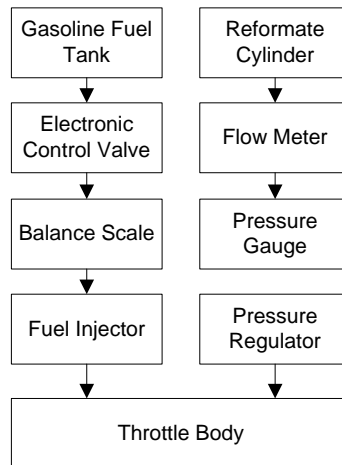


**Figure 6-2 Fuel supplied system**

### 6.3.1 Engine Fuel Replacement Calculation

The details relationship between reformat and equivalent fuel saving is explained in the following section.

### 6.3.2 Part I – Reformer Fuel Flow Calculation

In exhaust gas fuel reforming, several reforming reactions (Table 6-3) take place heterogeneously along the catalyst surface. The reaction's equilibrium depends largely on the exhaust gas temperature and reactants ratios (i.e.  $H_2O:C$ ,  $CO_2:C$  and  $O_2:C$ ), parameters that also significantly affect the overall reforming efficiency.

This section explains the calculations of the optimum fuel required in the reformer. As an example, when a 25L/min of engine exhaust is supplied to the reformer, given that Table 6-4 for the exhaust gas composition. From stoichiometric (mole:mole) calculations (see Table 6-3), fuel flow rates of 117, 166.5 and 55.5 ml/h are needed to maintain a stoichiometric  $H_2O:C$  ratio of 1 by SRR;  $CO_2:C$  ratio of 1 by DRR, and  $O_2:C$  ratio of 0.5 by POX, respectively. The sum of these individual fuel flow rates required (339 ml/h) can be considered as the highest fuel flow rate required for the optimum reforming efficiency. Note that the stoichiometry of complete combustion ( $O_2:C=1.46$ , Table 6-3 , COX) is undesired for the  $H_2$  or CO yield, therefore is not included.

**Table 6-3 Gasoline reforming reactions**

Reaction	Name of Reaction	Formula	Stoichiometry
1	SRR	$C_nH_{1.835n} + nH_2O \rightarrow nCO + 1.918nH_2$	H <sub>2</sub> O:C=1
2	DRR	$C_nH_{1.835n} + nCO_2 \rightarrow 2nCO + 1.835nH_2$	CO <sub>2</sub> :C=1
3	POX	$C_nH_{1.835n} + 0.5nO_2 \rightarrow nCO + 0.918nH_2$	O <sub>2</sub> :C=0.5
4	COX	$C_nH_{1.835n} + 1.459nO_2 \rightarrow nCO_2 + 0.918nH_2O$	O <sub>2</sub> :C=1.46

**Table 6-4 Exhaust gas composition**

CO	HC	CO <sub>2</sub>	O <sub>2</sub>	H <sub>2</sub>	H <sub>2</sub> O	N <sub>2</sub>
%	ppm	%	%	%	Calculated (%)	%
0.28	5224	13.1	2.4	0	12.48	71.22

### 6.3.3 Part II – Equivalent Engine Fuel Replacement

In order to define the equivalent engine fuel replacement from the reformat flow rate, the density changes due to the reforming process must be taken into consideration. Given the fact that N<sub>2</sub> is non-reactive in the reforming process, it can be used as a calibration factor to represent the changes in density of the reformat, i.e. the volumetric flow rate of N<sub>2</sub> at the inlet and outlet of the reformer is expected to be the same, see *Eq. 6.4-1* and *6.4-2*. As a consequence, for a 25 L/min of exhaust gas and 339 ml/h of gasoline that enter the reformer, a reformat flow rate of 31.9 L/min is produced. Based on this information, a projected equivalent engine fuel replacement is shown in Table 6-2. Note that any small changes in the engine exhaust composition when reformat is fed into the engine are assumed to be minimal in order to reduce the complexity of the calculations.

$$\text{Calibration Factor} = \frac{N2_{outlet}(\%)}{N2_{inlet}(\%)} \quad Eq. 6.4 - 1$$

$$\text{Flow Rate}_{\text{Reactor Outlet}} = \text{Flow Rate}_{\text{Reactor Inlet}} \times \text{Calibration Factor} \quad Eq. 6.4 - 2$$

## 6.4 Effect of Reformate on Combustion Performance

### 6.4.1 Mass Fraction Burn

Despite the reduced mass flow rate of air/Fuel mixture that goes into the engine, it is observed that from the 5% MFB, the combustion phase was advanced during the first 5 to 10% of MFB and became more noticeable with the increasing proportions of fuel replacement; see Figure 6-3 to Figure 6-5. This was mainly attributed to i) the low minimum ignition energy of hydrogen (i.e. 12 times lower relative to gasoline) and ii) the high laminar flame velocity (~3 m/s for hydrogen compared to ~0.4 m/s of gasoline). These results are supported by (Conte & Boulouchos, 2006) in their flame front studies of gasoline combustion with reformate additions using optical spark plug and ions sensors. They concluded that the laminar flame speed increases with the energy fraction of reformer gas in the gasoline fuel blend that mainly shortens the early phase of the combustion process. Also (Yu et al., 1986) reported a direct correlation between hydrogen and the increase in laminar flame speed during a hydrocarbon and air mixture combustion experiment. Besides, the reduction in vapour pressure required to vaporise any liquid fuel on combustion wall might had also contribute to this advance in combustion phasing. Therefore an attempt to retard the

ignition timing was conducted to each condition, by a fixed 4 CAD, intended to observe the effects on combustion behaviour. As a consequence, closer combustion phasing to the baseline MTB spark timing were observed, even though slightly over retarded, it has the effects of reducing the post combustion work on the compression stroke (Before TDC). The later phase of the combustion, i.e. 10 to 90% of MFB, generally follows the same trend and gradient with the baseline condition. This implies there are minimum effects on the combustion flame speed once the combustion is initiated due to the similarity in turbulent flame speeds between the reformat and gasoline, which again is reinforced by (Conte & Boulouchos, 2006) findings.

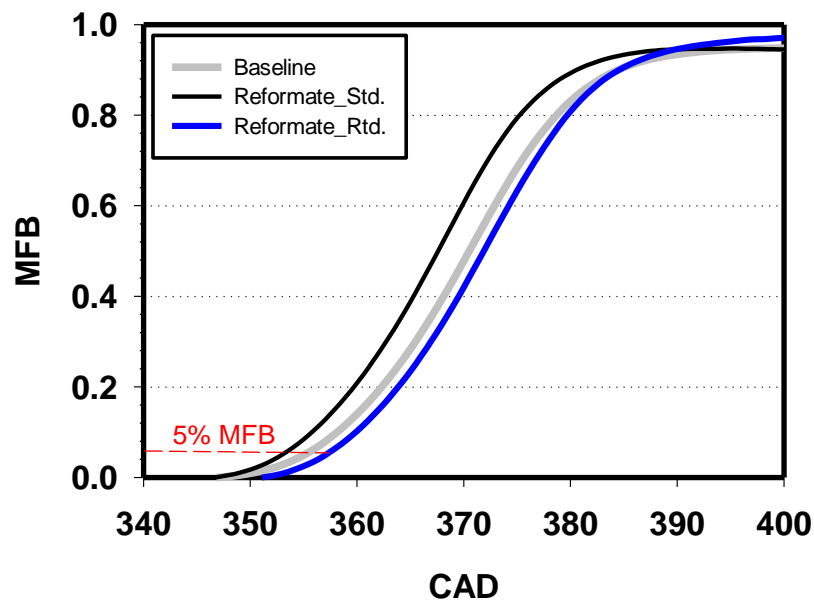


Figure 6-3 MFB at 18% fuel replacement

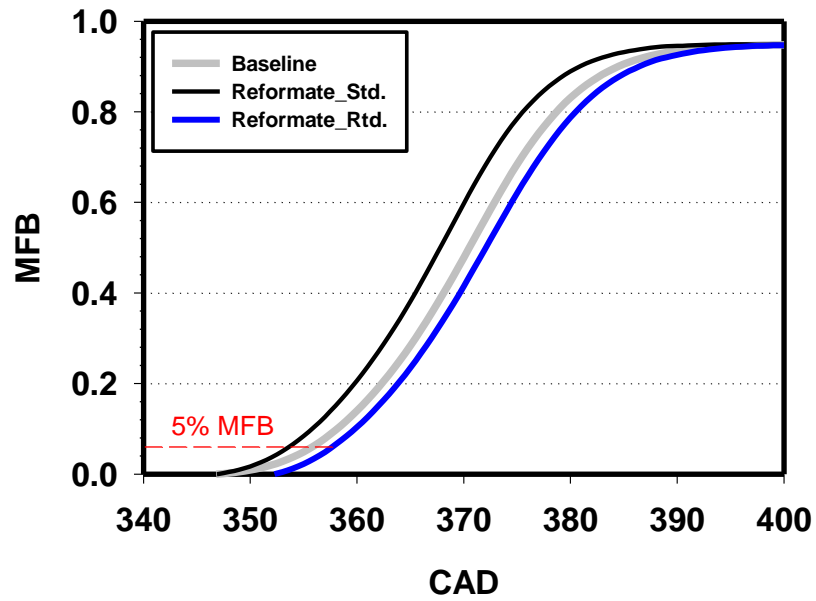


Figure 6-4 MFB at 23.9% fuel replacement

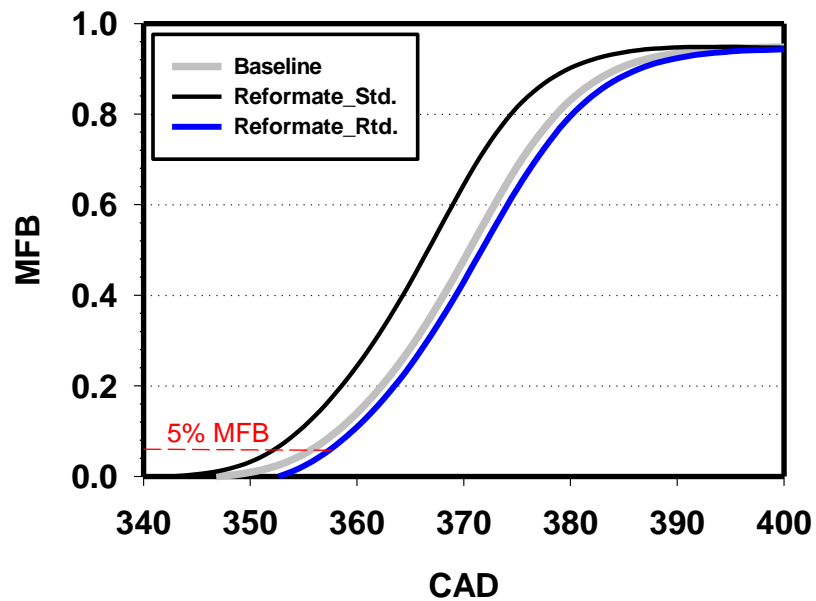


Figure 6-5 MFB at 29.9% fuel replacement

## 6.4.2 Combustion Stability

Combustion stability is mainly correlated to the combustion period available, as it provides more time to the flame front to influence the unburned mixture nearby.

Alternatively, enhancing in laminar velocity with reformat additions has the equivalent effect of extending the knock limit, meaning the compression ratio of such system could be extended to achieve higher combustion efficiency. As a result, positive effects on the combustion stability (represents as coefficient of variation of IMEP) with the increase reformat proportion as can be seen in Figure 6-6. It is worth noting that the increased usage of reformed (i.e. simulated REGR) did not associate with negative effects of conventional EGR, such as undesired combustion pattern (i.e. normal burn, slow burn, partial burn, and misfire), (Kuroda et al., 1978).

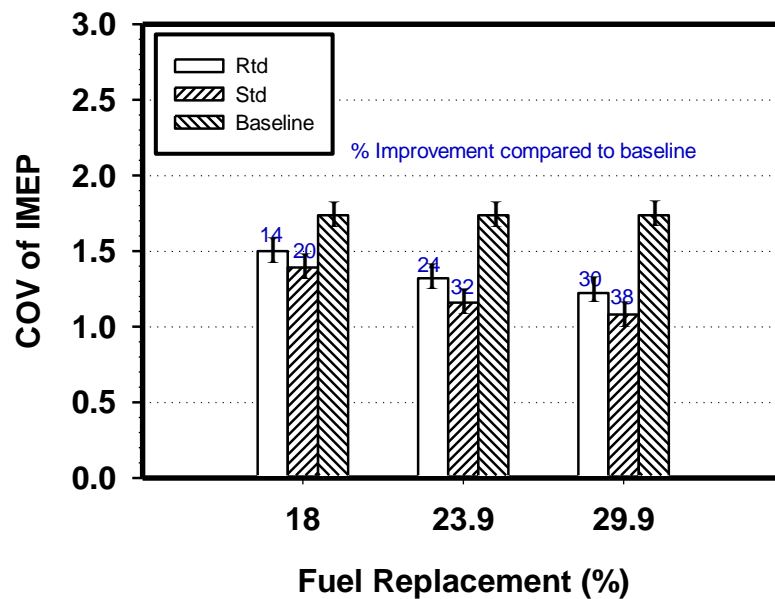


Figure 6-6 Effects of fuel replacement on COV of IMEP

### 6.4.3 Fuel Consumption

The fuel saving achieved by partially replacing gasoline by simulated reformat is

presented in Figure 6-7. It is found that the fuel saving is generally sensitive to spark timing when the fuel replacement is relatively low. At 18% fuel replacement, negative fuel savings have been observed in both standard (Std) and retarded (Rtd) spark timing due to over advanced (Adv) and over retarded spark timing respectively. At this specific condition, the 10-90% MBT (i.e. turbulent burning rate) with standard spark timing was noticeably shorter than the rest of the conditions. One likely explanation could be the increase in throttling position causing an increase in turbulence intensity in the unburned charge mixture, similarly to the effects with increased engine speed (Heywood, 1989). In contrast, the more turbulent combustion due to reformat addition became insignificant with rising proportion of fuel replacement. The observed fuel saving at 23.9 and 29.9% fuel replacement were higher than expected solely due to increased heating value, the observed fuel saving were 19.1 and 16.2% accordingly. This suggests both the chemical and dilution effects had co- contributed to the overall fuel saving. This is supported by the PMEP reduction shown in Figure 6-8.

(Ji & Wang, 2009) have conducted a dual fuelled (gasoline and hydrogen) experimental study on a SI engine at idle conditions. They observed a reduction in fuel consumption of 25.17 when 18.09% of H<sub>2</sub> was employed as a gasoline fuel replacement. More reports regarding hydrogen addition improving brake/indicated thermal efficiency can be found in (Apostolesu & Chiriac, 1996); (Varde, 1981).

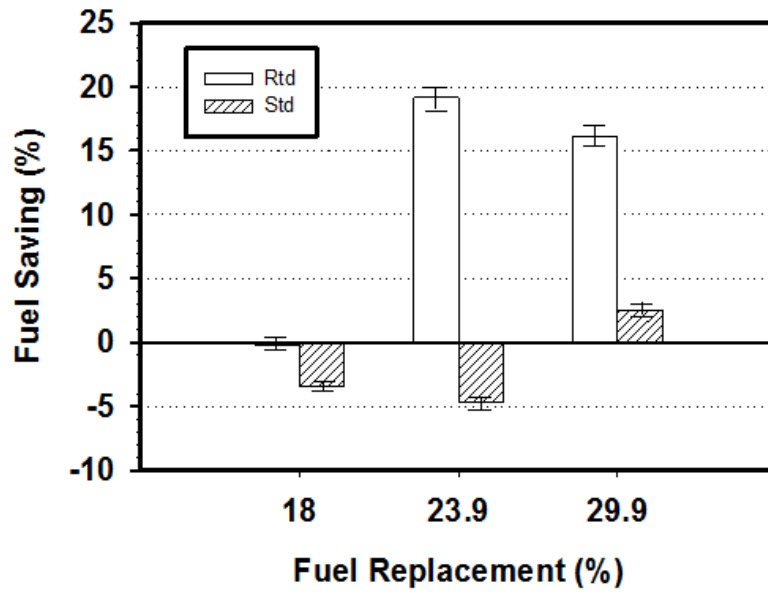


Figure 6-7 Effects of fuel replacement on fuel saving

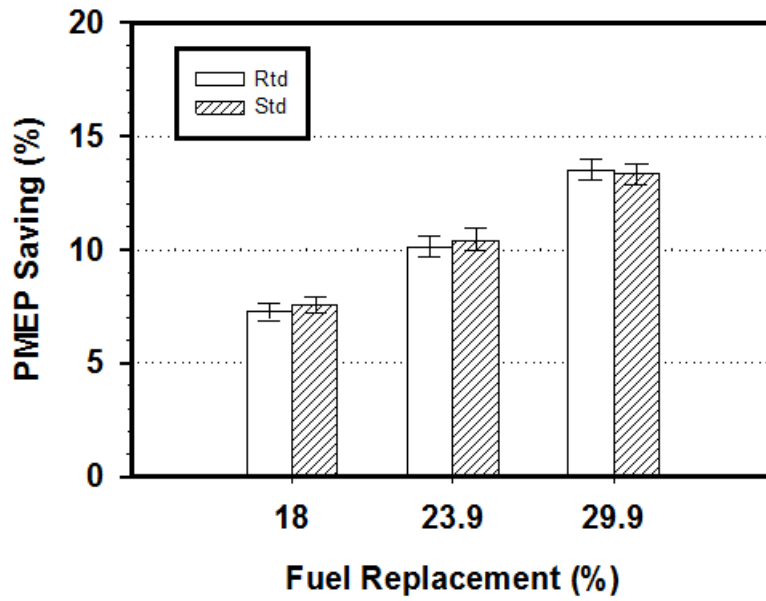
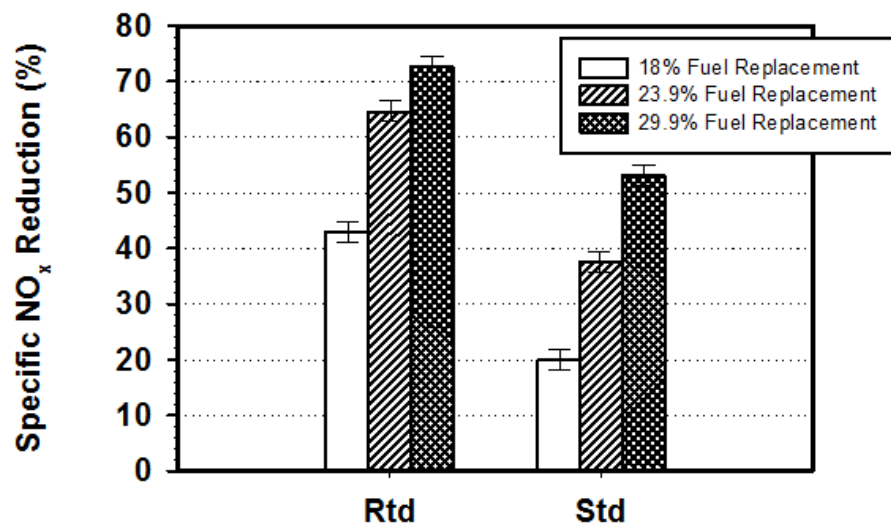


Figure 6-8 Effects of fuel replacement on pumping losses improvement

## 6.5 Engine out Emissions

The specific NO<sub>x</sub> emissions are presented in Figure 6-9. It can be seen that the addition of reformat improves specific NO<sub>x</sub> emissions significantly, in proportion with the

amount of fuel being replaced. This is a direct consequence of i) dilution effect that suppressed the max combustion temperature ii) the reduced specific fuel consumption. Without retarding the spark timing, NOx emissions benefit was primarily due to the earlier effect.



**Figure 6-9 Effects of fuel replacement on specific NOx reduction**

The hydrocarbon emissions are presented in Figure 6-10. It can be seen that the addition of reformat has significant effect on the level of emitted hydrocarbons. This reduction has previously been discussed and is attributed to the specific fuel economy and the fact that a significant amount of long chain hydrocarbon has been replaced by H<sub>2</sub>, CO and short chain HC. This also explains the positive HC reduction even when the specific fuel saving was negative. The same explanation can be applied to the improved in combustion stability.

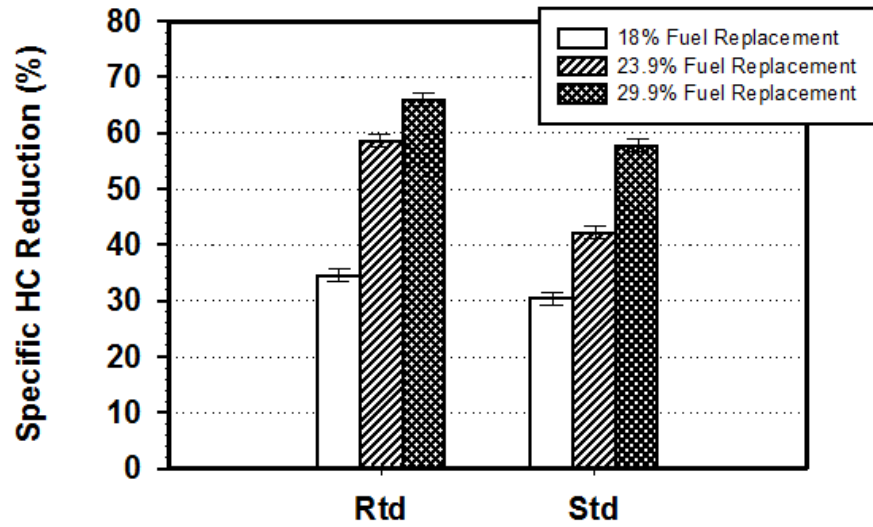


**Figure 6-10 Effects of fuel replacement on specific HC reduction**

The carbon monoxide emissions reduction is significant regardless of the fuel savings, Figure 6-11. This is attributed to the enhanced mixing offered by the reformat. This is also shown with the trend related to the spark timing; generally lowest emissions come from the retarded spark timing at 23.9% fuel replacement, similar to the maximum fuel saving condition.

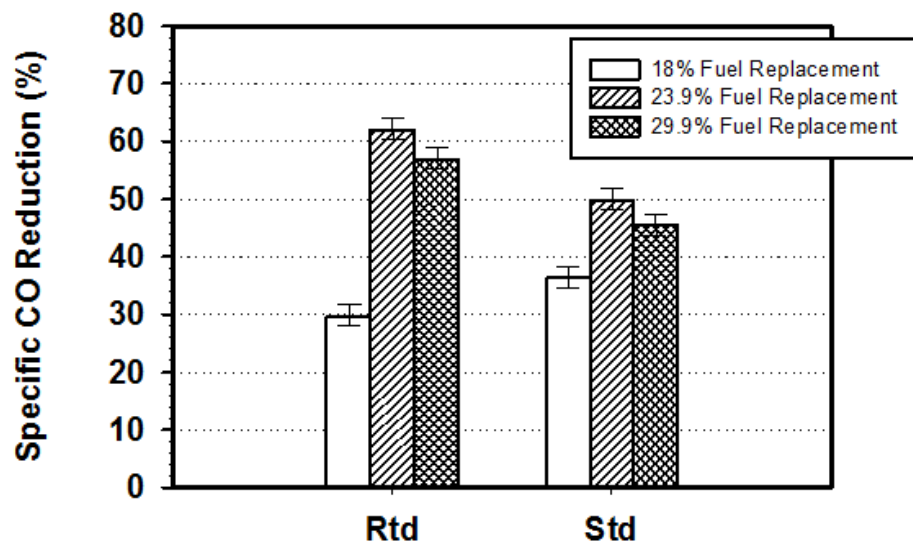


**Figure 6-11 Effects of fuel replacement on specific CO reduction**

Combustion efficiency (calculated from CO and HC in the exhaust stream) are presented in Figure 6-12. It can be seen that reformate addition enhanced the combustion efficiency closed to 100%, regardless of the spark timing and percentage of fuel replacement. This is reinforced by the reduction in unburned HC and CO emissions even when the fuel saving is negative in some cases. This can be attributed to the combined benefit of low coefficient of diffusion, low quenching gap and reduced heat of vaporisation of hydrogen over gasoline.

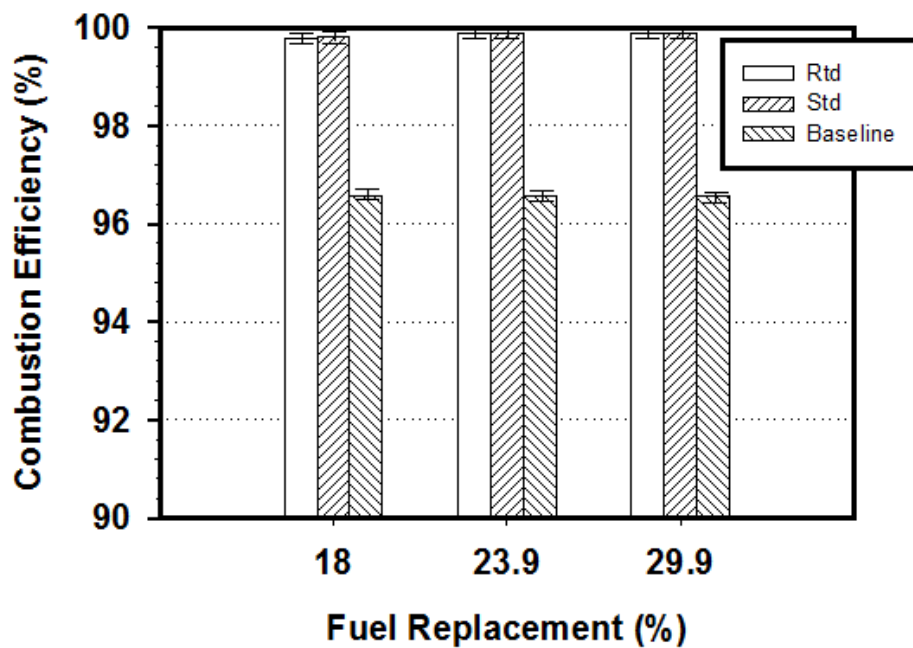


Figure 6-12 Effects of fuel replacement on combustion efficiency

# CHAPTER 7

## 7 Summary

A novel concept of utilising exhaust gas energy from a spark ignition engine to generate hydrogen onboard a vehicle and use it as a partial fuel replacement has been investigated. The feasibility of this technology has been studied in stages, covering i) the reforming catalyst operating window of major reforming reactions (i.e. dry reforming, steam reforming, water gas shift and partial oxidation) under simulated exhaust condition, ii) the reactor performance under actual gasoline exhaust gas conditions and iii) incorporate simulated reformat as a partial fuel replacement on a SI engine. The theoretical and actual fuel saving are compared via each stage.

*Chapter 4* - Several reactions can contribute to the overall process of exhaust gas reforming, during which some of the engine fuel is catalytically converted mainly to H<sub>2</sub> and CO. If the predominant reactions are endothermic, the process acts as a means of exhaust-heat recovery, and the fuel heating value is raised. When using conventional gasoline or diesel fuel, the reforming catalyst is required to promote steam- and dry-reforming, at the expense of the exothermic reactions-water gas shift, methanation, partial oxidation and combustion. In this study we show that a precious metal formulation is capable of catalysing most of the key reforming routes with the exception of the water gas shift reaction, under the

set of conditions that we have used to simulate an exhaust that we have used from a bioethanol-fuelled spark ignition engine. Our results at this stage predict that the overall process of exhaust gas reforming of  $C_2H_5OH$  will be oxidative, and yet waste heat will be consumed. The expected increase in fuel heating value is 6%, but can rise towards 20% if there is less  $O_2$  available in the exhaust, allowing more of the bioethanol to react by steam- and dry-reforming in the catalyst bed.

*Water Gas Shift*- is an undesired reaction in exhaust gas reforming, as it lowers the heating value of the reformat. It was observed that the catalyst performance fell short of the chemical equilibrium, but closely matched our kinetic model predictions that were based on published rate expressions for the forward and reverse shift reactions in a blank monolith. The  $H_2$  and  $CO_2$  concentrations vary from 0.2 to 1% vol. with exhaust temperature  $550^\circ$  to  $900^\circ C$ , accordingly, regardless of its S:CO ratios, the concern over WGS being over-active and negatively impacting the reformat heating value should therefore not be a concern.

*Steam Reforming* - is one of the most favourable reforming reactions in exhaust gas reforming, as its essential reactant (i.e. water) is always available within the SI engine exhaust. It was concluded that the catalyst is active towards steam reforming reaction; up to 122% of the overall efficiency has been achieved at  $800^\circ C$ , which is close to the theoretical efficiency of 127%. The expected  $H_2:CO$  product ratio has only become apparent at a narrow

temperature range between reactor temperature of 700° to 750°C, limiting the reaction of achieving 100% conversion. The likely explanation at temperatures below 700°C was due to side reactions and inter-particle diffusion.

In exhaust gas reforming, dry reforming is another reaction that favours hydrogen production which co-exists with steam reforming. It relies on fuel and carbon dioxide that are obtained from the engine exhaust as well as the product of steam reforming. In our results, a maximum efficiency of 111% has been observed, where the theoretical efficiency is 128%. Despite that SRR and DRR sharing a similar theoretical efficiency value, the fact that DRR is more endothermic means that a lower efficiency than SRR is expected at the same temperature. It was observed that the bioethanol conversion increases with rising exhaust temperature, the correlation between bioethanol conversion and CO<sub>2</sub>:F ratio only persists at temperatures below 700°C where there was an excess of CO<sub>2</sub> in the gas phase. A possible temperature poisoning by a temperature sensitive species has been observed between 800°-850°C, but recovered with further increased of temperature.

Partial Oxidation –results indicated that catalytic combustion (producing CO<sub>2</sub> and H<sub>2</sub>O), steam reforming (consuming the H<sub>2</sub>O formed) and dry reforming (consuming the CO<sub>2</sub> formed) took place consecutively in the catalyst bed as a function of temperature, with clearly some overlap across the temperature range. With steam reforming increasingly

dominating as a function of temperature and would therefore expected to continue to be the predominant endothermic reaction.

Chapter 5 - The same reforming catalyst has been tested under real exhaust gas conditions from a gasoline fuelled engine. The reforming catalyst showed no sign of deactivation or coking. The reformate product ratio coincided with the expected stoichiometric ratios of SRR and DRR reactions,  $H_2:CO$  of 1.92 and 0.92, respectively. Suggesting the gasoline reforming process is mainly dominated by SRR reaction at exhaust gas temperatures regime below  $750^\circ C$ , and DRR reaction for temperature above  $750^\circ C$ . At exhaust gas temperatures of  $950^\circ C$ , approximately 23% of the  $H_2$  production was achieved.

Based on the examined exhaust gas temperatures ( $600^\circ$  to  $950^\circ C$ ), the calorific value of the fuels during the fuel reforming process was improved and was in the range of 107 to 119%. Based on this results it was estimated that if 50% of the gasoline is being reformed, a realistic approximation of 3.6 to 9.4% fuel saving can be achieved when the engine is closed-couple with exhaust gas fuel reformer. These promising results are mainly contributed to the recovery of wasted exhaust heat which initiates the endothermic reforming reactions.

Chapter 6 - To conclude the study, the feasibility of close-looped onboard fuel reforming is continued, by replacing part of the gasoline fuel of the SI engine with simulated reformate. Studies using simulated reformate in a gasoline fuelled engine has been carried

out to examine what fuel economy benefits can be achieved. The composition of reformat was selected based on the previous exhaust gas fuel reforming experiment (e.g. test carried out at temperature of 850°C). The results suggest that up to 19% fuel savings can be achieved by replacing 23.9% of the gasoline with reformat. This remarkably high fuel savings is not only a result of the improved calorific value of the fuel but due to combined benefit of i) raising the fuel heating value, ii) reduced throttling restriction and iii) enhanced combustion efficiency. The fuel saving benefits however is sensitive to spark timing particularly when the fuel replacement is relatively low and required optimisation, ideally via feedback control. At 18% fuel replacement, negative fuel savings have been observed in both standard and retarded spark timing due to over advance and over retarded spark timing respectively.

Over the years, a number of research groups have explored the idea of exhaust gas fuel reforming, including the University of Birmingham, Cardiff University and University of Poitiers. This study is believed to be the first to demonstrate the potential fuel saving and simultaneous emission reduction on a spark ignition engine. Through the recovery of exhaust heat and recycling exhaust gas emissions, up to 19.1% fuel saving has been observed by replacing 23.9% gasoline with simulated reformat.

### Future work

So far, this study has been using bottled gas with known concentration of simulated reformat as a feedstock to engine. For the next stage of this study, the author would recommend replacing the simulated reformat with actual reformed product downstream of the reactor. This would allow the fuel saving under real closed-loop condition to be studied. Also, the transient response and light-off characteristics should also be considered as part of the future work, potentially recycling part of the reformat upstream of the reformer and possibly introduce oxygen into the reformer inlet so that exhaust temperature can be beneficial to by the oxidation along the catalyst.

The result in this study, fuel was injected as a large droplet using a medical syringe. Optimisation includes injector pressure, injector cone angle, spray pattern are all the potential elements to further improve the overall reformer efficiency.

Furthermore, to realise this reforming technology onboard an engine, the next stage of this project is to scale-up the prototype reformer which can be close coupled with the engine. Challenges including scaling-up the catalyst performance, and having good mass and heat transfer for maximum exhaust heat recovery, and precise fuel control strategy, are expected to be overcome.

## 8 LIST OF PUBLICATIONS

### Author Publications

Leung P., Tsolakis A., Golunski S., Rodriguez-Fernandez J., Golunski S., Raising the Fuel Heating Value and Recovering Exhaust Heat by On-board Oxidative Reforming of Bioethanol, The Royal Society of Chemistry, Energy & Environmental Science, 2010, 3, 780-788.

**Leung P.**, Tsolakis A., Golunski S., Wyszynski M. L., Gasoline Exhaust Gas Assisted Fuel Reforming as a Heat Recovery Technique, International Journal of Hydrogen, Article in Press.

**Leung P.**, Moolla I., Tsolakis A., Rajaram R. R., Collier J., Millington P., Pignion J., Thompsett D., Prototype Fuel Reformer Design Optimisation for On-Board Hydrogen Production, Article in-press

Hasan A. O., **Leung P.**, Tsolakis A., Xu H. M., Golunski S. E., Determination of Low Hydrocarbons Species (C1-C7) from HCCI/SI Gasoline Engine Equipped with Prototype Catalyst, Article in-press.

Piaszyk J., **P. Leung**, Wyszynski M. L., Tsolakis A., Williams B., Latham P., York A., Neat Tallow Combustion in a Large Diesel Engine for Electricity Generation from Waste, Energy & Fuels, 2012, 26, 12, 7069-7392.

Hasan A.O., **Leung P.**, Tsolakis A., Golunski S. E., Xu H. M., Wyszynski M. L., Richardson S., Effect of Composite Aftertreatment Catalyst on Alkane, Alkene and Monocyclic Aromatic Emissions from an HCCI/SI Gasoline Engine, Fuel, 2011, 90, 1457-1464.

Rounce P., Solakis A., **Leung P.**, York A. P. E., A Comparison of Diesel and Biodiesel Emissions using Dimethyl Carbonate as an Oxygenated Additive, Energy & Fuels, 2010, vol. 24, 4812-4819.

Sitshebo S., Tsolakis A., Theinnoi K., Rodriguez-Fernandez J., **P. Leung**, Improving The Low Temperature NO<sub>x</sub> Reduction Activity Over a Ag-Al<sub>2</sub>O<sub>3</sub> Catalyst, Chemical Engineering Journal, 2010, 158, 3, 402-410.

Hasan A. O., Mistzal J. W., Tsolakis A., Xu H. M., **Leung P.**, Golunski S., Richardson S., Control of HC, CO and NO<sub>x</sub> Emissions over a Prototype Catalyst in Gasoline Engine, Article in Press.

### **SAE Technical Publications and Presentation**

**Leung P.**, Tsolakis A., Wyszynski M. L., Rodriguez-Fernandez J., Megaritis A., Performance, Emissions and Exhaust-Gas Reforming of an Emulsified Fuel: A Comparative Study with Conventional Diesel Fuel, SAE Technical Paper, 2009-01-1809, Florence, Italy.

**Leung P.** and Tsolakis A., Hydrogen Production using Emulsified Diesel Exhaust Gas Reforming, International Symposium on Environment, Athens, Greece, 2009.

**Leung P.**, Tsolakis A. and Golunski S., Onboard Exhaust Gas Fuel Reforming, Catalyst Preparation 4<sup>th</sup> RSC & IChemE , 2010.

**Leung P.**, Exhaust Gas Heat Recovery to Achieved Fuel Saving on a S.I. Engine, UICEG, 2010

### **Awards**

1. Universitas 21 Doctoral Exchange Scholarship Award 2010
2. David Brewster Cobb Prize for Outstanding Automotive Publication 2010
3. Austin Rover Prize for Outstanding Automotive Publication 2009

## 9 REFERENCES

- 2009/30/EC Official Journal of the European Union. DIRECTIVES.  
On the Promotion of The Use of Energy from Renewable Sources and Amending  
and Subsequently Repealing Directives 2001/77/EC and 2003/30/EC
- Aardahi & Rassat, (2009) Aardahi C. L. and Rassat S. D. (2009) Overview of  
Systems Consideration for On-board Chemical Hydrogen Storage, **International  
Journal of Hydrogen Energy**, 34, 16, 6676-6683.
- Agnolucci (2007) Agnolucci P. (2007) Hydrogen Infrastructure for the  
Transport Sector, **International Journal of Hydrogen Energy**, 32: 15, 3526-  
3544
- Alger et al., 2007 Alger T., Gingrich J. and Mangold B. (2007) The Effect  
of Hydrogen Enrichment on EGR Tolerance in Spark Initied Engines. **SAE  
Technical Paper**, 10.4271/2007-01—475.
- Ahmed et al., 1998 Ahmed S., Krumpelt M., Jumar R., Lee S. H. D., Carter  
J. D., Wilkenhoener R. and Marshall C. (1998) Catalytic Partial Oxidation  
Reforming of Hydrocarbon Fuels, **Fuel Cell Seminar**. Palm Springs, CA.
- Anderson (2009) Anderson L. (2009) Ethanol Fuel Use in Brazil: Air  
Quality Impacts, **Energy Enviromental Science**, 10, 1015-1037.
- Andrews et al., 1988 Andrews G. E., Harris J. and Ounzain A. (1988)  
Transient Heating and Emissions of an SI Engine During the Warm-up Period.  
**SAE Technical Papers**, 880264.
- Ansell (1991) Ansell G. P., Golunski S. E., Hatcher H. A. and  
Rajaram R. R. (1991) Effects of SO<sub>2</sub> on Alkane Activity of Three-Way  
Catalysts, , 11, 183-190.
- Athanasios (2004) Athanasios N. Fatsikostas, Xenophon E. Verykios  
(2004) Reaction Network of Steam Reforming of Ethanol over Ni-based  
Catalysts, **Journal Catalysis**, 255: 2, 439-452.
- APEC (2008) **Asia-Pacific Economic Cooperation** (2008) APEC  
Biofuels Task Force Fifth Meeting, National Renewable Energy Laboratory.
- Apostolesu & Chiriac (1996) Apostolesu N. and Chiriac R. (1996) A study of  
Combustion of Hydrogen-enriched Gasoline in a Spark Ignition Engine, **SAE**

**Technical Paper**, 10.4271/960603.

- ASTM **American Society for Testing and Materials** (n.d.).  
STM D323 - 08 Standard Test Method for Vapor Pressure of Petroleum Products  
(Reid Method).
- Barbier (1994) J. Barbier and D. Duprez (1994) Steam Effects in 3-  
Way Catalyst, **Applied Catalyst B**, 4, 105-140.
- Bellido et al. 2009 Bellido J. D. A., Tanabe E. Y., Assaf E. M. (2009)  
Carbon Dioxide Reforming of Ethanol Over Ni/Y<sub>2</sub>O<sub>3</sub>-ZrO<sub>2</sub> Catalysts, **Applied  
Catalysis B**, 90, 485-488.
- Breen et al., 2002 Breen J., Burch R., and Coleman H. M. (2002) Metal-  
Catalysed Steam Reforming of Ethanol in the Production of Hydrogen for Fuel  
Cell Applications, **Applied Catalysis B: Environmental**, 39, 65-74.
- Burch et al., 1996 Burch R., Loader P. K., Cruise N. A. (1996) An  
Investigation of the Deactivation of Rh/alumina Catalysts Under Strong  
Oxidising Conditions, **Applied Catalysis**, 147, 2, 375-394.
- Bustamante et al., 2004 Bustamante F., Enick R. M., Cugini A. V., Killmeyer R.  
P., Howard B. H., Rothenberger K. S., Ciocco M. V., Morreale B. D.,  
Chattopadhyay S., and Shi S. (2004) High-Temperature Kinetics of the  
Homogeneous Reverse Water Gas shift reaction, **American Institute of Chemical  
Engineers**, 50, 1028-1041.
- Chammas and Paris (2005) Chammas E. and Paris E. M. (2005) Combined Cycle  
for Hybrid Vehicles. SAE World Congress & Exhibition, **SAE Technical Paper**,  
2005-01-1171.
- Cheng et al., 1993 Cheng W., Hamrin D., Heywood J.B., Hochgreb S.,  
Min K. and Norris M. (1993) An Overview of Hydrocarbon Emissions  
Mechanisms in Spark Ignition Engines, **SAE Technical Paper**, 932708.
- Choi & Stenger (2003) Choi Y. and Stenger G. (2003) Water Gas Shift  
Reaction Kinetics and Reactor Modeling for Fuel Cell Grade Hydrogen, **Journal  
of Power Sources**, 142, 2, 432-439.
- COM (2012) COM (2012) 595 Final, Directive of The European  
Parliament and of The Council, An EU Strategy for Biofuels. Brussels:  
Commission of the European Communities.

- Conte & Boulouchos (2006) Conte E. and Boulouchos K. (2006) Experimental Investigation into the Effect of Reformer Gas Addition on Flame Speed and Flame Front Propagation in Premixed Homogeneous-Charge Gasoline Engines, **Combustion and Flame**, 146, 329-347.
- Deluga (2004) Deluga G. A., Salge J. R., Schmidt L. D., and Verykios X. E. (2004) Renewable Hydrogen from Ethanol by Autothermal Reforming, **Science**, 303, 993-997.
- Diagne et al., 2002, Diagne C., Idriss H., and Kiennemann A. (2002) Hydrogen Production by Ethanol Reforming over Rh/CeO<sub>2</sub>-ZrO<sub>2</sub> catalysts, **Catalysis Communications**, 3: 12, 565-571.
- Edwards et al. (2008) Edwards P. P., Kuznetsov V. L., David W. I. F. and Brandon N. P. (2008) Hydrogen and Fuel Cells: Towards a Sustainable Energy Future. **Energy Policy**, 36, 12, 4356-4362.
- Elghawi et al., 2008 Elghawi U., Theinnoi K., Sitshebo S., Tsolakis A., Wyszynski M. L., Xu H.M., Cracknellb R. F., Clarkb R. H., and Mayoufc A. (2008) **International Journal of Hydrogen Energy**, 33, 23, 7074-7083.
- EPA. (1997) Environmental Protection Agency US (1997) Drinking Water Advisory: Consumer Acceptability Advice and Health Effects Analysis on Methyl Tertiary-Butyl Ether.
- EPA. (2010) Environmental Protection Agency US (2010) FY 2011 budget in brief
- EPA. (2011) Environmental Protection Agency US (2011) January 21. Federal Register, 76, 71.
- Ferguson & Kirkpatrick (2001) Ferguson C. and Kirkpatrick A. **Internal Combustion Engines Second Edition**. WILEY 2011
- Fisher (1999) Fisher G. B. (1999) NO<sub>x</sub> Reactivity Studies of Prototype Catalysts for a Plasma-Catalyst Aftertreatment System, **SAE Technical Paper**, 01-3685.
- Frusteri (2004) Frusteri F., Freni S., Spadaro L., Chiodo V., Bonura G., Donato S. and Cavallaro S. (2004) H<sub>2</sub> Production for MC Fuel Cell by Steam Reforming of Ethanol Over MgO Supported Pd, Rh, Ni and Co Catalysts, **Catalysis Communication**, 5, 611-615.

- Gallucci (2010) Gallucci F., Annaland M. V. S. and Kuipers J. A. M., (2010) Pure Hydrogen Production via Autothermal Reforming of Ethanol in a Fluidized Bed Membrane Reactor: A Simulation Study. **International Journal of Hydrogen Energy** 35, 1659-1668.
- Glassman (1996) Glassman I. (1996) Combustion Third Editions. San Diego: Academic Press.
- Green (2007) Green J.B. Jr., Domingo N., Storey J. M. E., Wagner R.M., Armfield J.S., Bromberg L., Cohn D. R., Rabinovich A., Alexeev N., (2007) Experimental Evaluation of SI Engine Operation Supplemented by Hydrogen Rich Gas from a Compact Plasma Boosted Reformer, **SAE Technical Paper**, 2000-01-2206.
- Guo (2004) Guo H., Smallwood G. J., Liu F., Ju Y., and Gulder O.L. (2004) The Effect of Hydrogen Addition on Flammability Limit and NO<sub>x</sub> Emission in Ultra-lean Counterflow CH<sub>4</sub>/Air Premixed Flames. **Proceedings of the Combustion Institute**, 30, 303-311.
- Harrington (1973) Harrington J. A. and Shishu R. C. (1973) A single-cylinder Engine Study of the Effects of Fuel Type, Fuel Stoichiometry, and Hydrogen-to-carbon Ratio on CO, NO, and HC Exhaust Emissions. **SAE Technical Paper**, 10/4271/730476.
- Haryanto (2007) Haryanto A., Fernando S. and Adhikari S. (2007) Ultrahigh Temperature Water Gas Shift Catalysts to Increase Hydrogen Yield from Biomass Gasification, **Catalysis Today**, 129: 3-4, 269-274.
- Hasan et al. (2011) Hasan A.O., Leung P., Tsolakis A., Golunski S.E., Xu H.M., Wyszynski M.L. and Richardson S. (2011) Effect of Composite Aftertreatment Catalyst on Alkane, Alkene and Monocyclic Aromatic Emissions from an HCCI/SI Gasoline Engine, **Fuel**, 90: 4, 1457-1764.
- Heywood (1989) Heywood J. B. (1989) Internal Combustion Engine Fundamentals, ISBN 0-07-100499-8 McGraw-Hill.
- Hira & Oliverira (2009) Hira A., and Oliverira L.G. (2009) No Substitute for Oil? How Brazil Developed its Ethanol Industry, **Energy Policy**, 37: 6, 2450-2456.
- Hoard (2001) Hoard J. (2001) Plasma-Catalyst for Diesel Exhaust

- Treatment: Current State of the Art, **SAE Technical Paper**, 01-0185.
- Holladay (2009) Holladay J. D., Hu J., King D. L. and Wang Y. (2009) An Overview of Hydrogen Production Technologies, **Catalysis Today**, 139, 4, 244-260.
- Hu & Lu (2009) Hu X. and Lu G. (2009) Syngas Production by CO<sub>2</sub> Reforming of Ethanol over Ni/Al<sub>2</sub>O<sub>3</sub> Catalyst, **Catalysis Communication**, 10, 1633-1637.
- Hu & Ruckenstein (2004) Hu Y. H. and Ruckenstein E. (2004) Catalytic Conversion of Methane to Synthesis Gas by Partial Oxidation and CO<sub>2</sub> Reforming, **Advance in Catalysis**, 48, 297-345.
- IEA (2010) **International Energy Agency** C. E. (2010) CO<sub>2</sub> emissions from fuel combustion highlight, 2010 edition.
- ITF (2010) **International Transport Forum** (2010) Reducing Transport Greenhouse Gas & Emissions, Trends & Data, Leijzig: OECD.
- Ji & Wang (2009) Ji C. and Wang S. (2009) Effect of Hydrogen Addition on the Idle Performance of a Spark Ignited Gasoline Engine at Stoichiometric Condition, **Intional Journal of Hydrogen Energy**, 34; 3546-3556.
- Ji & Wang (2009) Ji C. and Wang S. (2009) Progress and Recent Trends in Homogeneous Charge Compression Ignition (HCCI) Engines, **Intional Journal of Hydrogen Energy Combustion Science**, 35, 398-437.
- Kale (2010) Kale G. R. and Kulkarni B. D. (2010) Thermoneutral Point Analysis of Ethanol Dry Autothermal Reforming, **Chemical Engineering Journal**, 165, 864-873.
- Kee et al., 2007 Kee S. S., Shioji M., Mohammadi A., Niishi M. and Inoue Y. (2007) Knock Characteristics and Their Control with Hydrogen Injection Using a Rapid Compression/Expansion Machine. **SAE Technical Papers**, 2007-01-1829.
- Kikuchi et al. (2003) Kikuchi T., Ito S. and Nakayama Y. (2003) Piston Friction Analysis Using a Direct-Injection Single-Cylinder Gasoline Engine, **JSAE Review**, 24, 1, 53-58.
- Kito (2000) Kito S., Wakai K., Takahashi S., Fukaya N. and Takada Y. (2000) Ignition Limit of Lean Mixture by Hydrogen Flame Jet Ignition, **JSAE**

**Review**, 21, 3, 393-378.

- Klouz (2002) Klouz V., Fierro V., Denton P., Katz H., Lisse J. P., Bouvot-Mauduit S. and Mirodatos C. (2002) Ethanol Reforming for Hydrogen Production in a Hybrid Electric Vehicle: Process Optimisation, **Power Sources**, 105, 1, 26-34.
- Kolb (2008) Kolb G. (2008) Fuel Processing for Fuel Cells, Wiley-VCH; 1 edition.
- Kuroda (1978) Kuroda H., Yucesu H. S., Nakajima Y., Sugihara K., Takagi Y., and Muranaka S. (1978), **SAE Technical Paper**, 780006.
- Lee et al., 2010 Lee D. H., Lee J.S., and Park J. S. (2010) Effects of Secondary Combustion on Efficiencies and Emission Reduction in the Diesel Engine Exhaust Heat Recovery System. **Applied Energy**, 87, 5, 1716-1721.
- Liguras (2003) Liguras D. K., Kondarides D. I. and Verykios X. E. (2003) Production of Hydrogen for Fuel Cells by Steam Reforming of Ethanol over Supported Noble Metal Catalysts, **Applied Catalysis B: Environmental**, 43, 345-354.
- Masaki & Asia Times (2007) Masaki & Asia Times. (2007) Japan Steps Up Its Biofuels Drive. Tokyo: **Asia Times Online Ltd.**
- Mack et al., 2009 Mack J. H., Aceves S. M. and Dibble R. W (2009) Direct Use of Wet Ethanol in a Homogenous Charge Compression Ignition (HCCI) Engine, **Energy**, 34, 6, 782-787.
- Martins et al., 2011 Martins J., Goncalves L., Antunes J. and Brito F. (2011) Thermoelectric Exhaust Energy Recovery with Temperature Control through Heat Pipes. **SAE Technical Paper**, 2011-01-0315.
- Mei (1979) Mei V. (1979) A Truck Exhaust Gas Operated Absorption Refrigeration System. **ASHRAE Transactions** 85, 66-67.
- Messerer et al. (2007) Messerer A., Schmatloch V., Poschl U. and Niessner R. (2007) Combined Particle Emissions Reduction and Heat Recovery from Combustion Exhaust, **Biomass and Bioenergy**, 31: 7, 512-521.
- Milpied et al., 2009 Milpied J., Jeuland N., Plassat G. and Guichaous S. (2009) Impact of Fuel Properties on the Performance and Knock Behaviour of a Downsized Turbocharged diesel Engine - Focus on Octane Numbers and Latent

- Heat of Vaporization. **SAE Technical Paper**, 10.427/2009-01-0324.
- Nadim (2001) Nadim F., Zack P., Hoag G. E. and Liu S. (2001) United States Experience with Gasoline Additives. **Energy Policy**, 29, 1, 1-5.
- Palmas et al., 2006 Palmas S., Ferrara F., Vacca A., Mascia M., Polcaro A. M. (2006) Behavior of Cobalt Oxide Electrodes during Oxidative Processes in Alkaline Medium, **Electrochimica Acta**, 53, 2, 400-406.
- Petitpasa (2007) Petitpasa G., Rollier J. D., Darmon A., Gonzalez-Aguilar J., Metkemeijer R. and Fulcheri L. (2007) A Comparative Study of Non-thermal Plasma Assisted Reforming Technologies, **International Journal of Hydrogen Energy**, 32, 14, 2848-2867.
- Piel & Thomas (1990) Piel W. J. and Thomas R. X. (1990) Oxygenates For Reformulated Gasoline, **Hydrocarbon Processing**, 18, 68-73.
- Pulkrabek (1997) Pulkrabek W. W. (1997) Engineering Fundamentals of the Internal Combustion Engine. In W. W. Pulkrabek. Prentice Hall.
- Rounce et al. Rounce P., Tsolakis A., Rodriguez-Fernandez J., York A. (2009) Diesel Engine Performance and Emissions when First Generation Meets Next Generation Biodiesel, **SAE Technical Paper**, 2009-01-1935.
- Satterfield (1996) Satterfield C. N. Heterogeneous Catalysis in Industrial Practice, Florida: Krieger Publishnig.
- Schoenung (2001) Schoenung S. M. (2001) Hydrogen Vehicle Fueling Alternatives: an Analysis Developed for the International Energy Agency, **SAE Technical Papers**, 2001-01-2528.
- Severin et al., 2005 Severin C., Pischinger S. and Ogrewalla J. (2005) Compact Gasoline Fuel Processor for Passenger Vehicle APU, **Journal of Power Sources**, 145, 675-682.
- Shinagawa et al. (2004) Shinagawa T., Okumura T., Furuno S. and Kim K. (2004) Effects of Hydrogen Addition to SI Engine on Knock Behavior, **SAE Technical Paper**, 10.4271/2004-01-1851.
- Simplicio et al., 2009 Simplicio L. M. T., Brandao S. T., Domingos D., Bozon-Verduraz F. and Sales E. A. (2009) Catalytic Combustion of Methane at High Temperatures: Cerium Effect on PdO/Al<sub>2</sub>O<sub>3</sub> Catalysts, **Applied Catalysis**, 360, 2-7.



- Ethanol for Hydrogen Production: Thermaodynamic Investigation, *International Journal of Hydrogen Energy*, 34, 13, 5382-5389.
- Wang et al., 2008                      Wang K., Li W.S., Zhou, X.P. (2008) Hydrogen Generation by Direct Decomposition of Hydrocarbons Over Molten Magnesium, *Journal of Molecular Catalysis. A, Chemical*, 283, 153-157.
- Yao (2009)                                Yao M., Zheng Z. and Liu H. (2009) Progress and Recent Trends in Homogenous Charge Compression Ignition (HCCI) Engines, *Progress in Energy Combustion Science*, 35, 5, 398-437.
- Yu et al., 1986                          Yu G., Law C. K. and Wu C. K. (1986) Laminar Flame Speeds of Hydrocarbon + Air Mixtures with Hydrogen Addition. *Combustion and Flame*, 63, 339-347.
- Yücesu (2006)                          Yücesu H. S., Topgül T., Çinar C. and Okur M. (2006), Effect of Ethanol-gasoline Blends on Engine Performance and Exhaust Emissions in Different Compression Ratios, *Applied Thermal Engineering*, 26, 17-18, 2272–2278.
- Zeldovich et al., 1947                Oxidation of nitrogen in combustion (trans. by M. Shelef), *Academy of sciences of USSR*.